

**150-m Measurement of 0.880- to 100.0-keV
Neutron Transmissions Through
Four Samples of ^{238}U**

D. K. Olsen
G. de Saussure
R. B. Perez
F. C. Difilippo
R. W. Ingle
H. Weaver

OAK RIDGE NATIONAL LABORATORY

OPERATED BY UNION CARBIDE CORPORATION FOR THE ENERGY RESEARCH AND DEVELOPMENT ADMINISTRATION

Printed in the United States of America. Available from
National Technical Information Service
U.S. Department of Commerce
5285 Port Royal Road, Springfield, Virginia 22161
Price: Printed Copy \$5.25; Microfiche \$3.00

This report was prepared as an account of work sponsored by the United States Government. Neither the United States nor the Energy Research and Development Administration, nor any of their employees, nor any of their contractors, subcontractors, or their employees, makes any warranty, express or implied, or assumes any legal liability or responsibility for the accuracy, completeness or usefulness of any information, apparatus, product or process disclosed, or represents that its use would not infringe privately owned rights.

ORNL/TM-5915
(ENDF-255)
Dist. Category UC-79d

Contract No. W-7405-eng-26
Neutron Physics Division

150-m MEASUREMENT OF 0.880- to 100.0-keV NEUTRON TRANSMISSIONS
THROUGH FOUR SAMPLES OF ^{238}U

D. K. Olsen, G. de Saussure, R. B. Perez,
F. C. Difilippo,* R. W. Ingle,** and H. Weaver

*On assignment from Comisión Nacional de Energía Atómica, Argentina.
**Instrumentation and Controls Division.

Date Published - October 1977

Prepared by the
OAK RIDGE NATIONAL LABORATORY
Oak Ridge, Tennessee 37830
operated by
UNION CARBIDE CORPORATION
for the
DEPARTMENT OF ENERGY

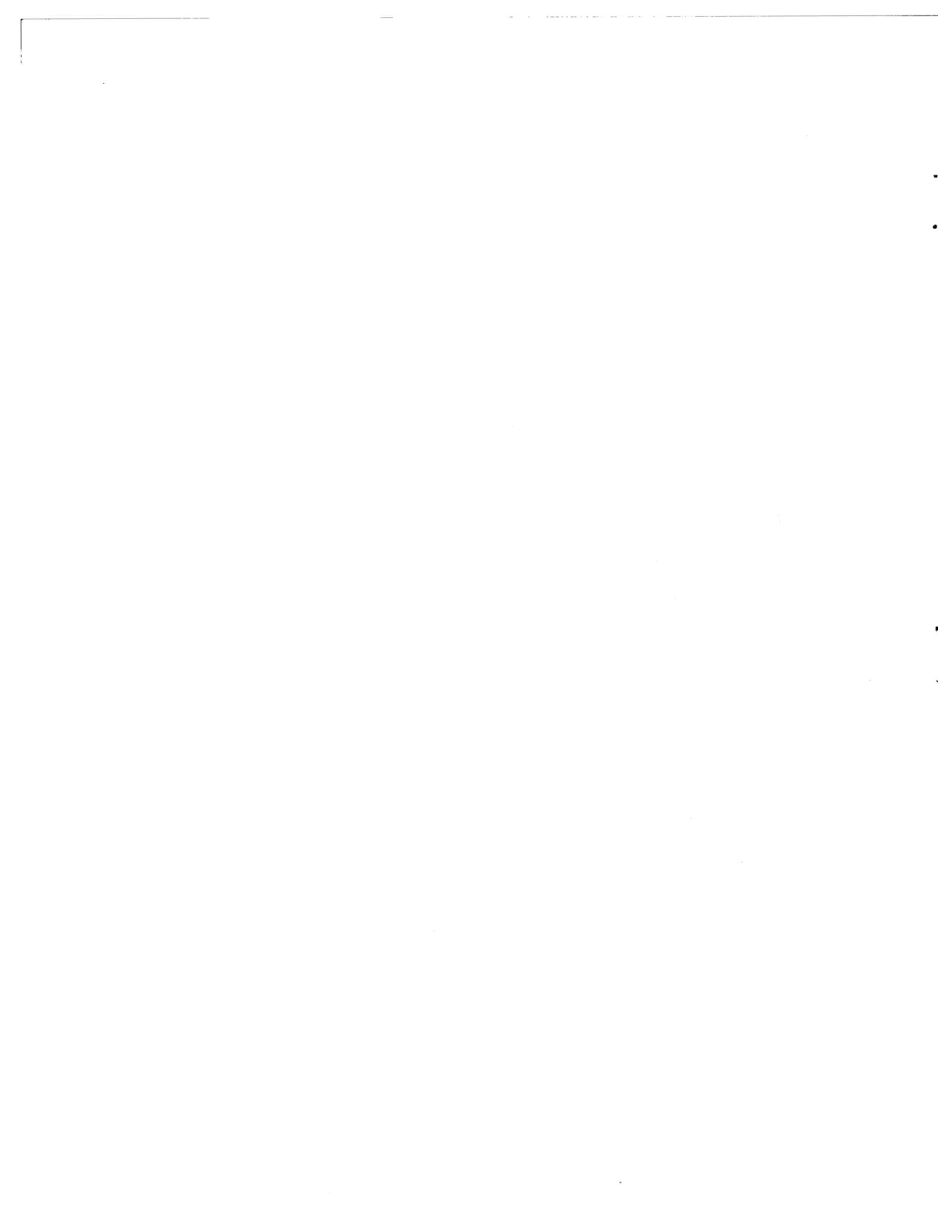
[Illegible text at the top of the page]

[Illegible text in the middle section of the page]

[Illegible text at the bottom of the page]

TABLE OF CONTENTS

	<u>Page</u>
ABSTRACT	ix
I. INTRODUCTION	1
II. EXPERIMENTAL APPARATUS AND PROCEDURE	6
1. <u>Beam Line</u>	6
2. <u>Detector and Electronics</u>	9
3. <u>^{238}U Samples</u>	11
4. <u>The Measurements</u>	13
III. DATA REDUCTION	15
1. <u>Energy Scale</u>	15
2. <u>Dead-Time Correction</u>	16
3. <u>Background Subtraction</u>	16
4. <u>Transmission Calculation</u>	19
IV. RESULTS AND DISCUSSION	21
1. <u>The Transmissions</u>	21
2. <u>Discussion of Uncertainties</u>	35
V. ACKNOWLEDGMENTS	39
REFERENCES	40
APPENDIX	42

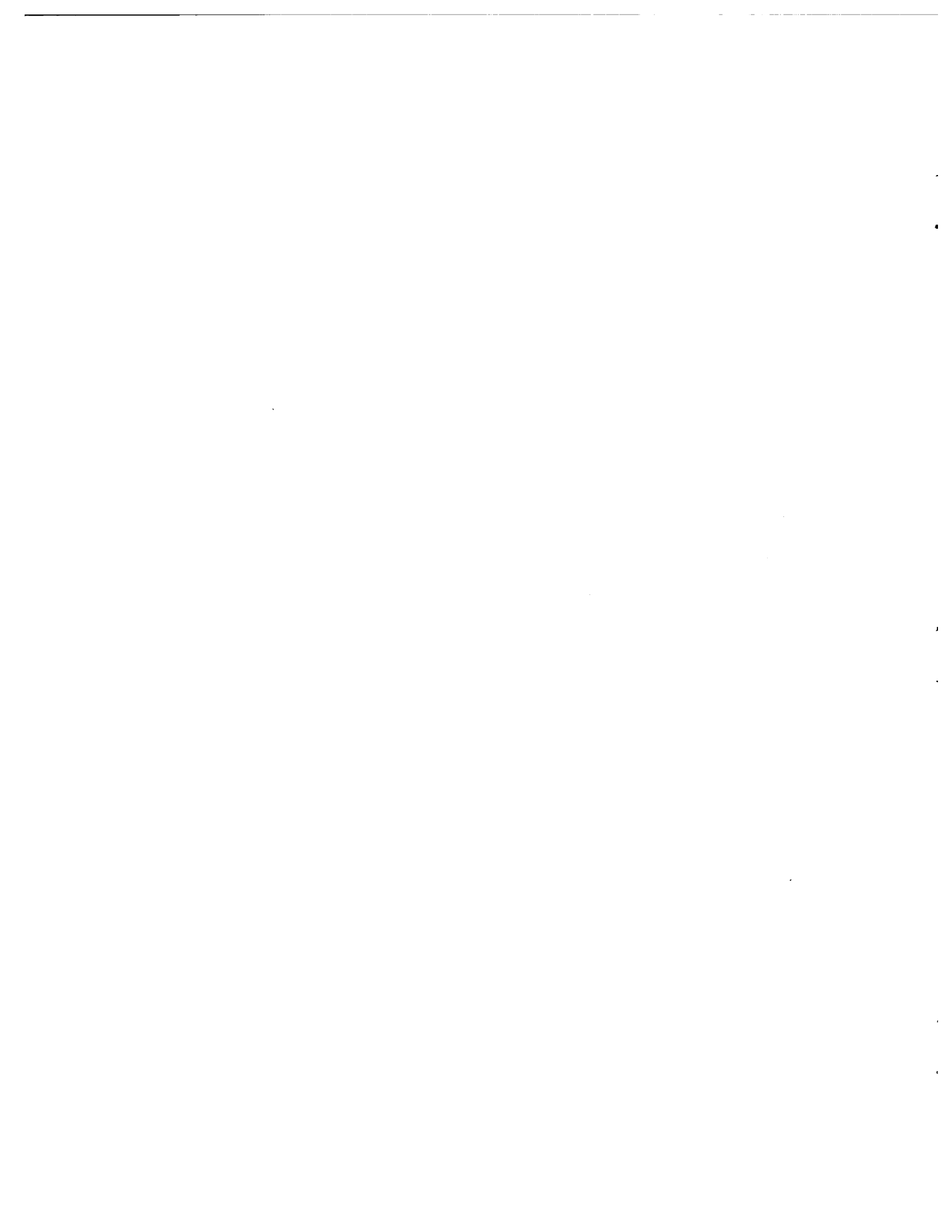


LIST OF FIGURES

	<u>Page</u>
1. Comparison of Local s-wave Strength Functions	3
2. ORELA Target-Moderator Assembly	7
3. Major Components of Data Acquisition System	10
4. ORELA Flux through 10.2 cm of Polyethylene	17
5. 0.254- and 3.62-cm Transmissions from 1 to 2 keV	22
6. 0.254- and 3.62-cm Transmissions from 2 to 3 keV	23
7. 0.254- and 3.62-cm Transmissions from 3 to 4 keV	24
8. 0.254- and 3.62-cm Transmissions from 4 to 6 keV	25
9. 0.254- and 3.62-cm Transmissions from 6 to 8 keV	26
10. 0.254- and 3.62-cm Transmissions from 8 to 12 keV	27
11. 0.254- and 3.62-cm Transmissions from 12 to 16 keV	28
12. 0.254- and 3.62-cm Transmissions from 16 to 20 keV	29
13. 1.08- and 3.62-cm Transmissions from 20 to 30 keV	30
14. 1.08- and 3.62-cm Transmissions from 30 to 40 keV	31
15. 1.08- and 3.62-cm Transmissions from 40 to 70 keV	32
16. 1.08- and 3.62-cm Transmissions from 70 to 100 keV	33
17. Average Cross Sections	36

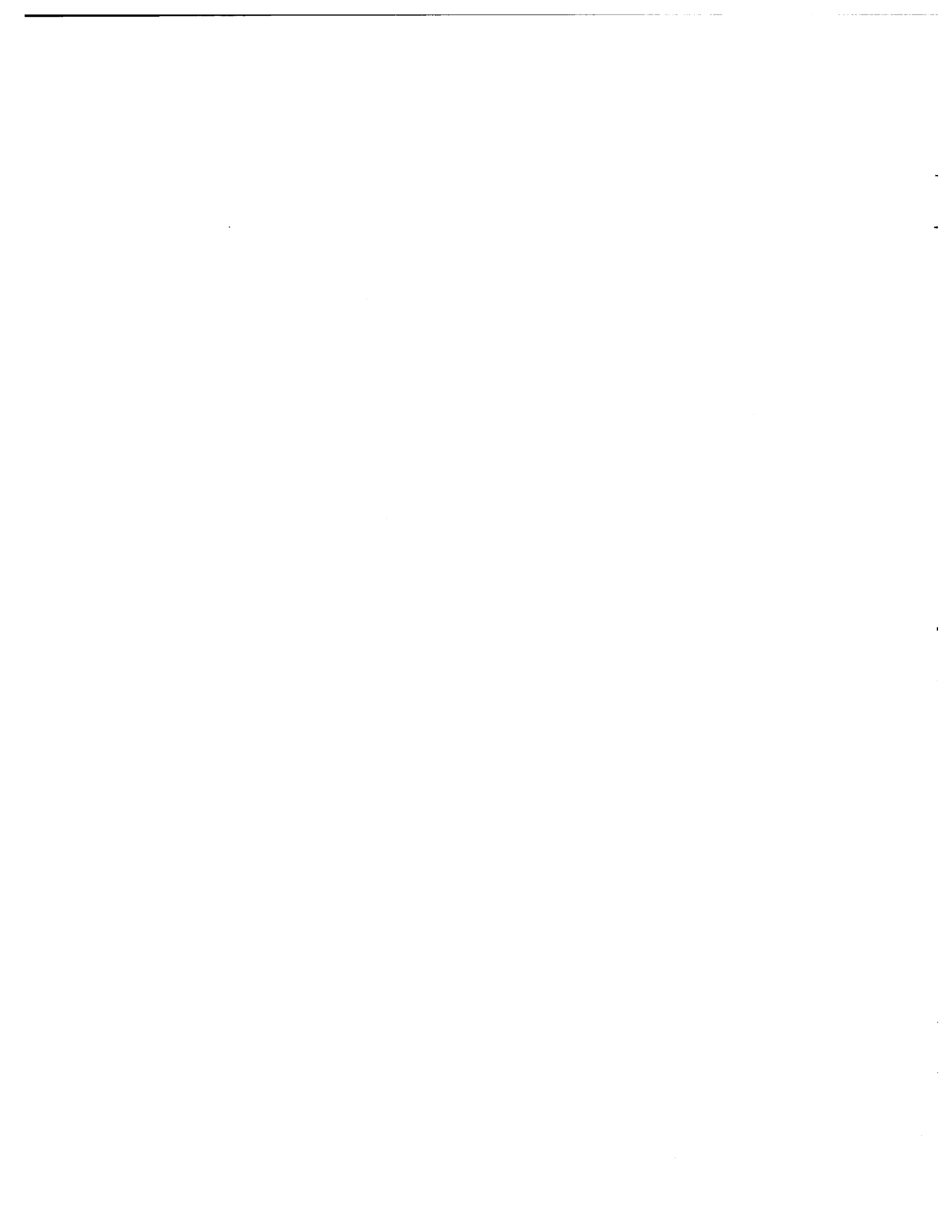
LIST OF TABLES

	<u>Page</u>
I. Other Transmission Measurements	4
II. ORELA Neutron Beam Conditions	8
III. Flight-Time Channel Structure	11
IV. ^{238}U Disk Used in the Measurement	12
V. ^{238}U Samples Used in the Measurement	12
VI. Beam Filters Used in the Measurement	14
VII. Beam Burst Per Measured Spectrum	14
VIII. Percentage Background Components	20
IX. Examples of Internal Consistency	37
X. Comparison Between 150-m and 40-m Cross Sections	38



ABSTRACT

In order to study the $^{238}\text{U}+n$ total cross section, neutron transmissions through 0.076-, 0.254-, 1.080-, and 3.620-cm-thick samples of isotopically enriched ^{238}U have been measured from 0.880 to 100.0 keV using a time-of-flight technique over a path length of 150 meters with the ORELA pulsed source and a 13-mm-thick Li-glass detector. The measurement is described in detail and both a listing and figures of the resulting transmissions are given. An absolute energy scale accurate to 2 parts in 10,000 was established.



I. INTRODUCTION

Because accurate total and partial neutron cross sections for ^{238}U are important for nuclear reactor design, these cross sections have been extensively investigated over the years. In the resolved resonance region, nominally energies below 4.0 keV, the neutron resonances are well separated and can be experimentally resolved; consequently, measured cross sections at these energies have been described in terms of individual resonance parameters. This parameterization allows these cross sections to be reconstructed at different temperatures, allows the calculation of self-shielding factors, and allows the determination of average resonance parameters. These average parameters form the bases for cross section calculations at energies where the individual resonances affect reactor performance, but cannot be experimentally resolved. In the ENDF/B-IV compilation for ^{238}U , this unresolved resonance range spans neutron energies from the resolved range to 45 keV.

Herein we report on the measurement from 0.880 to 100.0 keV of the total cross section of ^{238}U from neutron transmissions through 0.076-, 0.254-, 1.080-, and 3.620-cm samples. In principle the measurement is simple. A pulsed neutron flux from the Oak Ridge Electron Linear Accelerator (ORELA) was collimated onto a 13-mm-thick Li-glass detector at 150 m. This detector measured the product of the neutron flux and detector efficiency as a function of neutron flight time. At 42 meters, ^{238}U samples were cycled in and out of the beam. Assuming a constant flux with the sample-in time equal to the sample-out time, the transmission $T_n(E)$ is simply the ratio of the sample-in flux to the sample-out flux. The measurement involves only a flux ratio; no knowledge of the neutron flux or detector efficiency is required. Assuming no resolution broadening, the Doppler-broadened cross section would be given by $\sigma(E) = -\ln[T_n(E)]/n$ where n is the nuclei per unit area of the sample.

However, the resolution broadening considerably complicates the analysis of the data because it acts on the transmission and not the cross section. Consequently, resonance parameters are obtained directly from

the transmissions, either with an area analysis or least-squares shape-fitting. The parameters usually obtained from such analyses are neutron widths, resonance energies, and the potential scattering radius. The neutron widths are both the most important and most difficult results to obtain accurately.

The need for an additional high-resolution ^{238}U transmission measurement is apparent from Fig. 1. In this figure the s-wave strength function — the summed reduced neutron widths divided by the corresponding energy interval — from various measurements is plotted for 0.5-keV intervals. Five total cross section measurements of the resolved region up to 4.0 keV have been published.¹⁻⁵ Details of these measurements are listed in Table I. Because the strength function of Garg *et al.*,¹ the earliest measurement, is systematically much smaller than those from the recent measurements, it is not shown in Fig. 1. The transmissions of Olsen *et al.*⁶ were only analyzed up to 1.087 keV and Nakajima *et al.*⁴ do not list neutron widths for many resonances in the 2.5- to 3.0-keV range. Below 1.5 keV the various measurements give neutron widths which average to strength functions in reasonable agreement. From 1.5 keV to 4.0 keV the measurements or analyses are discrepant. In particular, the strength function of Rahn *et al.*³ is systematically smaller than that of Carraro and Kolar,² 23% smaller from 3.5 to 4.0 keV. A strength function intermediate between these was obtained by Nakajima *et al.*,⁴ whereas the very recent results of Poortmans *et al.*⁵ support the large strength function of Carraro and Kolar.² The expected⁷ 5% precision for ^{238}U neutron widths has not been achieved, even when averaged into strength functions.

With increasing neutron energy the extracted neutron widths and resulting strength function become more and more unreliable because the average natural resonance width, the Doppler width, and the resolution width all increase whereas the level spacing remains approximately constant. This problem is expected to lead at high energies to an underestimation of the strength function which for ^{238}U is based on neutron widths below 4.0 keV. Nevertheless, Fig. 1 shows the measured values above 4.0 keV. The three²⁻⁴ reported sets of neutron widths in the 4.0-

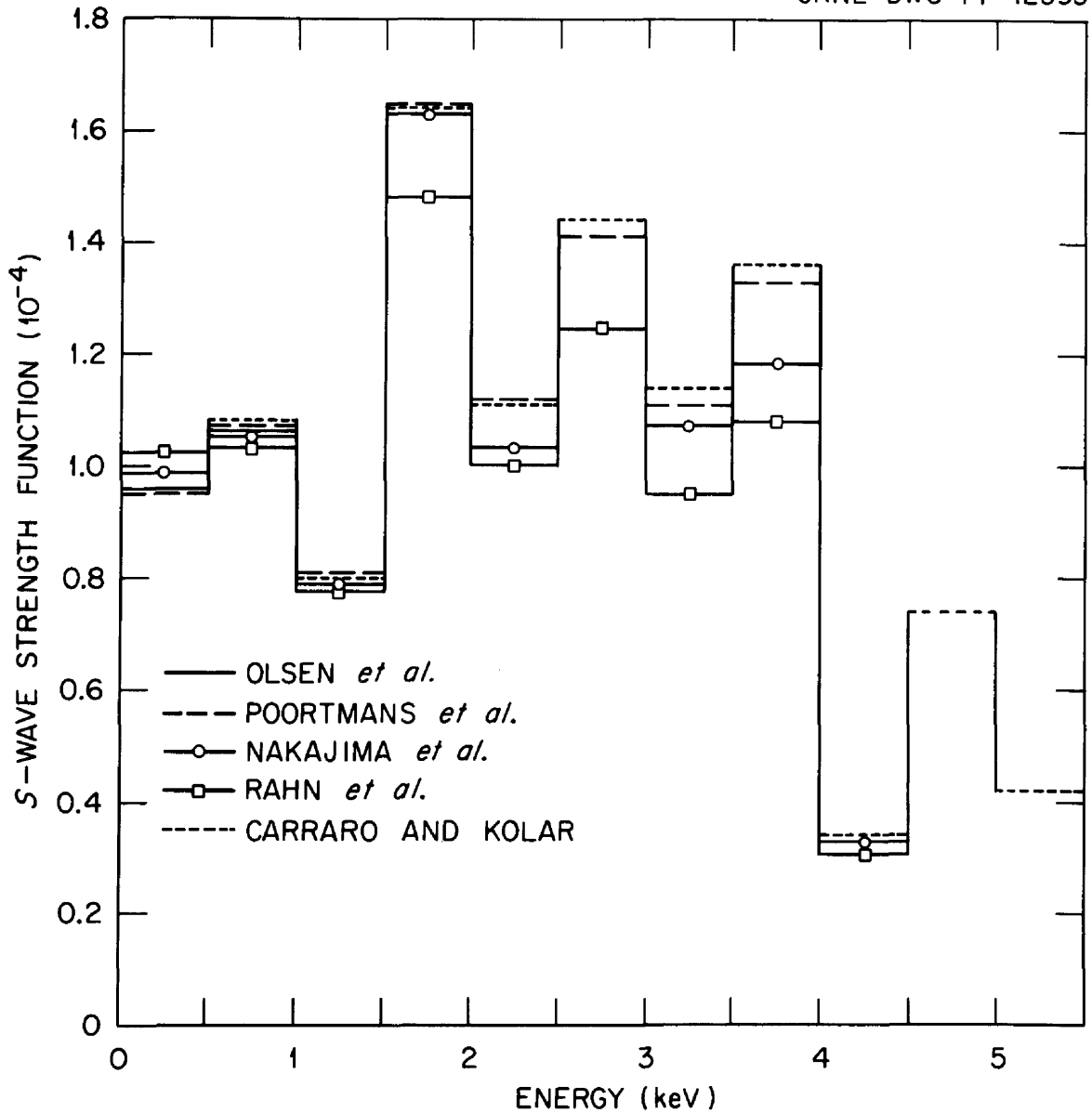


Fig. 1. Comparison of neutron widths on average employing local s-wave strength functions calculated for 0.5-keV intervals from a consistent set of levels for the various measurements of Refs. 2-6.

TABLE I. ^{238}U Transmission Measurements

Experimenters	Ref	Energy (eV)	Detector	Samples (barns/atom)	Neutron Source
Garg <i>et al.</i> (1964)	1	45 to 4000	$\text{NaI-}^{10}\text{B}$	590 235 150	Columbia synchrocyclotron 200 m
Carraro and Kolar (1970)	2	60 to 5700	$\text{NaI-}^{10}\text{B}$	155 91	Geel CBNM, electron linac, 100 m
Rahn <i>et al.</i> (1972)	3	6 to 4600	$\text{NaI-}^{10}\text{B}$	200 m 478 119 28.8 11.9	Columbia synchrocyclotron 40 m
Nakajima <i>et al.</i> (1974)	4	20 to 4662	13 mm Li-glass	138 69 at 77°K 42	JAERI electron linac, 190 m
Poortmans <i>et al.</i> (1977)	5	1 to 4270	^3He gas scintillator	13368 621 264	Geel CBNM electron linac 30 m and 60 m
Olsen <i>et al.</i> (1977)	6	1/2 to 1088	1 mm Li-glass	5404 1613 807 266	ORELA, 40 m

to 4.5-keV interval all agree on an exceedingly small strength function. At even higher energies only the measurements of Carraro and Kolar² have been analyzed. If the strength function above 4.0 keV is indeed as small as indicated by Fig. 1, its average value from the resolved range would perhaps require reduction which in turn would affect cross section calculation for the unresolved range.

The primary purpose of the present work is to obtain accurate transmissions from which reliable neutron widths can be extracted, both above and below 4.0 keV. A secondary goal is to provide total cross section information in the unresolved resonance range where presently there exists a dearth of measurements.⁸

This work is an extension of the previous 40-m measurement⁶ which was analyzed only up to 1.087 keV. Above this energy neutron widths from the various samples of this earlier work were discrepant, which seemed to indicate the need for more accurate measurements. The present transmissions are an improvement over the former transmissions in several ways.

- 1) The flight-path length was increased from 40 m to 150 m improving, in principle, the resolution by over a factor of three.
- 2) A ¹⁰B time-overlap filter was used removing the low energy Cd resonances which confused the previous 40-m spectra.
- 3) An absolute energy scale was established, whereas the 40-m energy scale was relative to resonance energies measured by others.
- 4) The open beam and four ²³⁸U samples were alternated in and out of the flux for 20 continuous days, whereas the 40-m work consisted of summing many half-day transmission measurements, each with its own open beam sampling. This new procedure assures a common energy scale, resolution function, background source, normalization, and open beam for the four transmissions.

The next section of this report describes the experimental apparatus and procedures. The section following explains the data reduction to transmissions and the last section illustrates and lists these results.

II. EXPERIMENTAL APPARATUS AND PROCEDURE

1. Beam Line

The measurements were performed on flight path number 6 of ORELA. Eight hundred pulses per second of approximately 140-MeV electrons were incident on the water-cooled tantalum target⁹ shown in Fig. 2. Slowing down in the tantalum plates these electrons produced bremsstrahlung which in turn produced fast neutrons from (γ, n) reactions. These fast neutrons were moderated down to lower energies by the target cooling water which was contained in a beryllium can with 2.4-mm-thick walls as shown. Average beam parameters and other conditions of the measurement are listed in Table II.

Between the target-moderator assembly and the Li-glass detector the beam passed through a manually operated filter changer, an automatic sample changer, and six collimators. The six collimators designated A, B, C, D, E, and F were located 2.5, 5.7, 17.6, 37.2, 79.4, and 149.5 m respectively from the target, had minimum circular apertures of 14.75, 13.93, 13.03, 10.57, 11.27, and 7.76 cm respectively, and produced a neutron beam with a 7.6-cm-dia umbra and 8.4-cm-dia penumbra at the 155-m detector position. The beam line was perpendicular to and viewed the entire target face except for the tantalum center which was shielded with 5.1- x 5.1- x 76.8-cm copper and lead rectangular shadow bar placed along the axis of collimator A. At the 5-m station, between collimators A and B, a 10-unit positioner for beam filters was located. The ^{238}U disks were mounted in a computer-controlled sample changer located a few meters beyond collimator D in the 40-m station. The beam entrance to the sample changer contained an additional Pb collimator which was 12.7 cm long and 9.2 cm in diameter.

The beam line was evacuated except for the sample changer and apparatus in the 150-m station. The sample changer required a 0.5-m air gap which was separated from the vacuum with .63 mm aluminum foils. The beam line in the 150-m station was filled with helium except for two air gaps with a total length of about 1.5 m and separated from the vacua

ORNL DWG 67-1012A

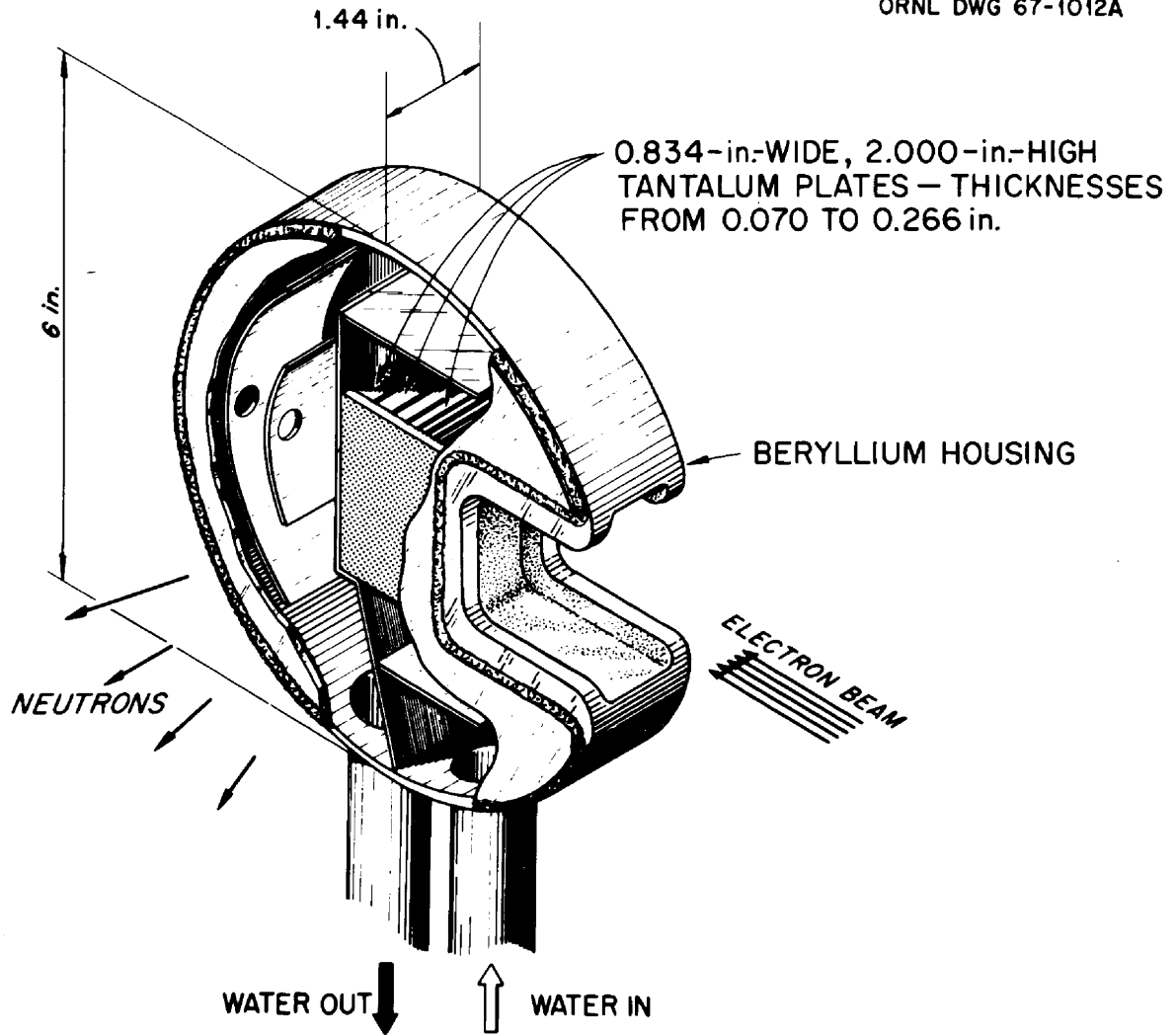


Fig. 2. ORELA Be clad tantalum target assembly.

TABLE II. Neutron Beam Parameters for ORELA
150-m ^{238}U Transmission Measurements

Flight Path	155.4 m
Moderator Composition	H_2O
Moderator Thickness	3.2 cm
Beam Bursts per Second	800
Electron Beam Power (time averaged)	20 kW
Electron Beam Burst Width	12 nsec
Sample Temperature	$294 \pm 3^\circ\text{K}$
Overlap Filter	$1.53 \text{ g/cm}^2 \text{ }^{10}\text{B}$

with 0.25-mm mylar foils. Those neutrons which passed through the ^6Li detector and the photomultiplier tube and base were stopped in lithium-paraffin blocks 9 m beyond the detector at the end of flight path number 6. A more complete description of the beam line is given in Ref. 10.

A distance from the neutron producing target to the detector is required for an absolute energy calibration. The distance from the center of the target-moderator assembly to the center of the Li-glass detector was determined to be 155441 ± 6 mm, which is the sum of two measurements. First, the slope distance from the center of the target to the interior face of the east concrete wall of the 150-m station at the beam line center had been measured by accurate surveying to be 150013 ± 4 mm.¹¹ Second, the distance from this point to the center of the Li-glass detector was measured with a steel tape to be 5428 ± 4 mm. The errors on these two measurements were added in quadrature.

2. Detector and Electronics

Neutrons were detected with an 11.1-cm-diameter, 12.7-mm-thick, ^6Li -loaded glass scintillator¹² whose face was optically coupled with a ~13-mm-thick quartz light pipe to an RCA-4522 phototube operated at -2300 volts. The detection efficiency of this detector was about 15% for 1.0-keV neutrons and assuming no self shielding was proportional to the $^6\text{Li}(n,\alpha)t$ cross section. The scintillator, light pipe, phototube, and base were all mounted in the neutron beam.

Figure 3 shows a block diagram of the electronic apparatus used to measure the time-of-flight spectra. Both the fast (anode) and slow (dynode) pulse from the photomultiplier base were amplified with bias levels set on the slow pulses and the timing performed with the fast pulses. The usual fast-slow coincidence signaled the detection of a neutron. Care was taken to ensure that the gamma-flash did not distort the pulse-height spectrum for times corresponding to energies below 100 keV. Neutron times-of-flight were measured with an E.G. & G. TDC-100 multistop time digitizer which measured the time interval between a start pulse and the fast-slow coincidence pulse. Start signals were obtained from a "gamma-flash" detector¹³ triggered by bremsstrahlung from the electron burst striking the ORELA target. The timing resolution of the neutron detector and associated electronics was about 2 nsec.

Various filter-sample configurations were alternated in and out of the neutron beam with an SEL-810B computer controlled sample changer where the beam-in time for each configuration was determined by requiring a fixed number of processed Li-glass events. The resulting flight-time spectra were constructed on a large-capacity, rapid, random-access magnetic disk attached to the SEL-810B computer. Each of the ten flight-time spectra required 52,250 timing channels. Table III gives the flight-time channel structure. An approximate measure ($\pm 10\%$) of the relative average neutron flux was obtained using the "house monitor" which consisted of a ^{235}U fission chamber wall mounted in the ORELA target room.¹⁴ For each sample-filter configuration of each cycle the total monitor counts, beam bursts, and Li-glass events were automatically recorded with computer-controlled scalars.

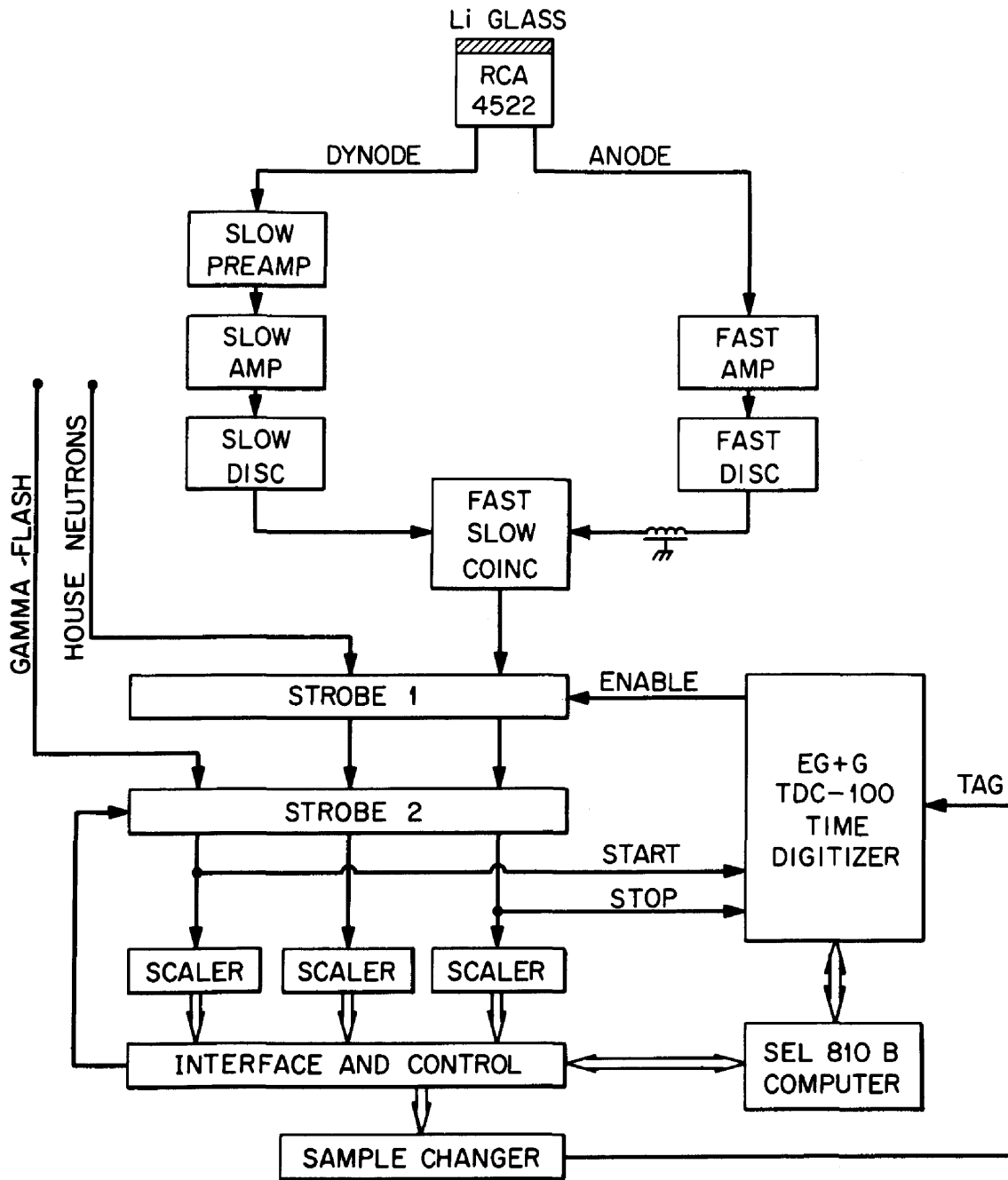


Fig. 3. Major components of data acquisition system.

TABLE III. Flight-Time Channel Structure for ORELA,
150-m ^{238}U Transmission Measurements

Number of Channels	Channel Width (nsec)	Time of Flight Range (μsec)	Energy Range (eV)
750	40	0 \rightarrow 30	00 \rightarrow 169438.
22500	4	30 \rightarrow 120	169436. \rightarrow 9178.1
10000	8	120 \rightarrow 200	9178.1 \rightarrow 3244.2
6250	16	200 \rightarrow 300	3244.2 \rightarrow 1428.8
6250	32	300 \rightarrow 500	1428.8 \rightarrow 510.7
4000	64	500 \rightarrow 756	510.7 \rightarrow 222.6
2500	128	756 \rightarrow 1076	222.6 \rightarrow 109.6

3. ^{238}U Samples

Transmissions were measured through 0.076-, 0.254-, 1.080-, and 3.620-cm-thick samples formed from 0.076-, 0.254-, 0.381-, 0.445-, and 2.540-cm-thick disks. The precise mean areal density and isotopic composition of each disk are given in Table IV. The 0.076- and 0.254-cm samples consisted of a single disk, the 1.080-cm sample consisted of the 0.254-, 0.381-, and 0.445-cm disks, and the 3.620-cm sample consisted of the 2.540-cm disk and the 1.080-cm sample. Table V gives the mean thickness of these samples with an estimate of the variation in thicknesses over the areas of the disk. The errors in the mean sample thickness are negligible. The sides of each disk were coated with $0.0012 \pm 0.0006 \text{ g/cm}^2$ of acrylic laquer¹⁵ to reduce oxidation and corrosion.

TABLE IV. Disks of ^{238}U for ORELA, 150-m Transmission Measurements

Nominal Thickness (cm)	Diameter (cm)	Areal Density (g/cm ²)	% Isotopic Composition			
			^{238}U	^{236}U	^{235}U	^{234}U
2.540 ^a	11.13	48.56	99.920	0.012	0.042	0.026
0.445 ^a	11.10	8.556	>99.9994	-	-	-
0.381 ^a	11.09	7.176	99.9991	-	0.0009	-
0.254 ^a	11.11	4.902	99.920	0.012	0.042	0.026
0.076 ^a	11.12	1.484	99.920	0.012	0.042	0.026

^aEach side coated with 0.0012 ± 0.0006 g/cm² of acrylic lacquer (9.1% hydrogen content by weight).

TABLE V. Samples of ^{238}U for ORELA 150-m Transmission Measurements

Nominal Thickness (cm)	Thickness (atoms/barn)	Thickness Variation (atoms/barn)	Inverse Thickness (barns/atom)
3.620	0.17536	0.0013	5.70
1.080	0.05208	0.0012	19.2
0.254	0.01239	0.00012	80.7
0.076	0.003760	0.00008	266

4. The Measurement

Table VI describes the five 16.5-cm-diameter beam filters employed in the measurements. The ^{10}B prevented time overlap of the neutron flux from successive bursts and the Pb attenuated the γ -flash to a tolerable level. The Al, Mn, and NaF filters were used to help determine background levels, both as a function of neutron energy and, more importantly, as a function of ^{238}U sample thickness.

Final data were taken with a continuous 20-day measurement cycling the ^{238}U samples and Al-Mn filter combination in and out of the beam with the 40-m sample changer. The duration of a complete data cycle was about 30 minutes and consisted of transmissions through the four ^{238}U samples followed by an open beam measurement, with each of these samples immediately repeated with the Al-Mn filter in the beam. Table VII lists the number of beam bursts for each sample-filter combination. More information on the background was provided by an additional two-day measurement which consisted of cycling 10.2 cm of polyethylene, 7.6 cm of polyethylene, the 0.254-cm ^{238}U sample, the NaF filter, the Al-Mn filter combination, and an open beam. The transmission through the polyethylene determined the γ -ray component of the background and the NaF filter provided additional black resonances for the overall background subtraction.

The time-independent beam off background was measured to be 7.3 cts/sec. Finally, the clock time of the centroid of the gamma-flash group was measured to be 3210 ± 2 nsec. This time is used to determine the zero point on the clock timing scale which is required for an absolute energy calibration.

TABLE VI. The 16.5-cm-Diameter Beam Filters for
ORELA 150-m ^{238}U Transmission Measurements

Function	Filter	Areal Density
Overlap	328 g $^{10}\text{B}^{\text{a}}$	1.53 g/cm 2 ^{10}B
γ -flash	6.4 mm Pb	7.21 g/cm 2 Pb
Background	2.54 cm Al	6.86 g/cm 2 Al
Background	46.8 g Mn $^{\text{b}}$.219 g/cm 2 Mn
Background	300 g NaF $^{\text{c}}$	1.40 g/cm 2 NaF

$^{\text{a}}$ In epoxy binder

$^{\text{b}}$ In 0.981 g/cm 2 S binder

$^{\text{c}}$ In 0.935 g/cm 2 S binder

TABLE VII. Total Number of Beam Bursts Used for
Each Sample-Filter Measurement

^{238}U Sample	Filters	10^6 Beam Burst
0.076 cm	open	108.477
0.076 cm	Al-Mn	37.887
0.254 cm	open	119.486
0.254 cm	Al-Mn	41.889
1.080 cm	open	159.048
1.080 cm	Al-Mn	65.452
3.620 cm	open	265.414
3.620 cm	Al-Mn	88.893
open	open	103.689
open	Al-Mn	35.996

III. DATA REDUCTION

Various transmission spectra were determined from the flight-time spectra through the ten sample-filter combinations. This data reduction required the calculation of an overall energy scale and a deadtime correction and background subtraction for each spectrum. From these corrected spectra, transmissions were calculated through the four ^{238}U samples both with and without the Al-Mn filter and through the Al-Mn filter with and without the various ^{238}U samples. This redundancy of transmission information provided some indication of the systematic uncertainty inherent in the measurement. The steps of the data reduction are described below.

1. Energy Scale

The nonrelativistic neutron energy E' in eV is related to the "clock" flight time t in nsec and a path length L in mm by the equation

$$E' = [72.2977L/(t-t_0)]^2, \quad (1)$$

where t_0 establishes the zero point on the "clock" timing scale. The measured distance of 155441 ± 6 mm from the target-moderator center to the detector center is used for L in Eq. (1). Use of this distance implies a moderation time equivalent to an increase in flight path length of 16 mm, the distance from the target center to the moderator face. Also it assumes that the $^6\text{Li}(n,\alpha)$ reactions on average occur at the center of the Li-glass disk. Because of these assumptions and to account for other systematic errors, the uncertainty for L was increased from ± 6 mm to ± 16 mm.

Gamma rays travel 155441 mm in 518.1 nsec; consequently, the gamma-flash "clock" time of 3210 ± 2 nsec required $t_0 = 2695 \pm 2$ nsec. The flight time of the channel center was used to calculate the channel energy.

In addition, the first order relativistic correction

$$E = E'(1 + 1.5965 \times 10^{-9}E') \quad (2)$$

was applied where E and E' were the relativistic and nonrelativistic energies respectively. A more complete discussion of the energy scale for this measurement can be found in ref. 16.

2. Dead-Time Correction

A fixed non-extending dead time of 8264 nsec, larger than the dead time of any of the electronic components, was artificially imposed on the counting system. Assuming the same neutron flux in each beam burst permitted a straightforward calculation of the dead-time correction using the equation

$$C_i^* = C_i \left[1 - \frac{1}{T} \sum_j C_j \right]^{-1}, \quad (3)$$

where C_i is the measured events in channel i , C_i^* is the dead-time-corrected events in channel i , T is the total ORELA beam bursts for the measurement, and the summation runs over all those channels j which preceded channel i by less than 8264 nsec. The dead-time correction never exceeded 8.00% for neutron energies less than 100 keV.

3. Background Subtraction

The background was divided into flight-time-independent and flight-time-dependent components with its subtraction proceeding from the known to the unknown. First, the counting rate of the detector system in situ was measured to be 7.3 cts/sec with the ORELA flux off. This flight time independent room background was subtracted from the ten spectra.

Next, the transmissions through the 7.6- and 10.2-cm thick polyethylene samples were analyzed in order to determine the gamma-ray admixture measured in the neutron flux. Figure 4 shows the 10.2-cm transmission where the smooth curve is a visual fit using both a flight-time-independent and flight-time exponential decay terms. Below 100 keV, 7.6 cm of polyethylene effectively attenuates neutrons but not gamma rays. The exponential decaying background has a half-life of 18.4 μ sec, is 2.23-MeV radiation from hydrogen capture in the water moderator, is well understood,¹⁷ and is a significant background at high energies.

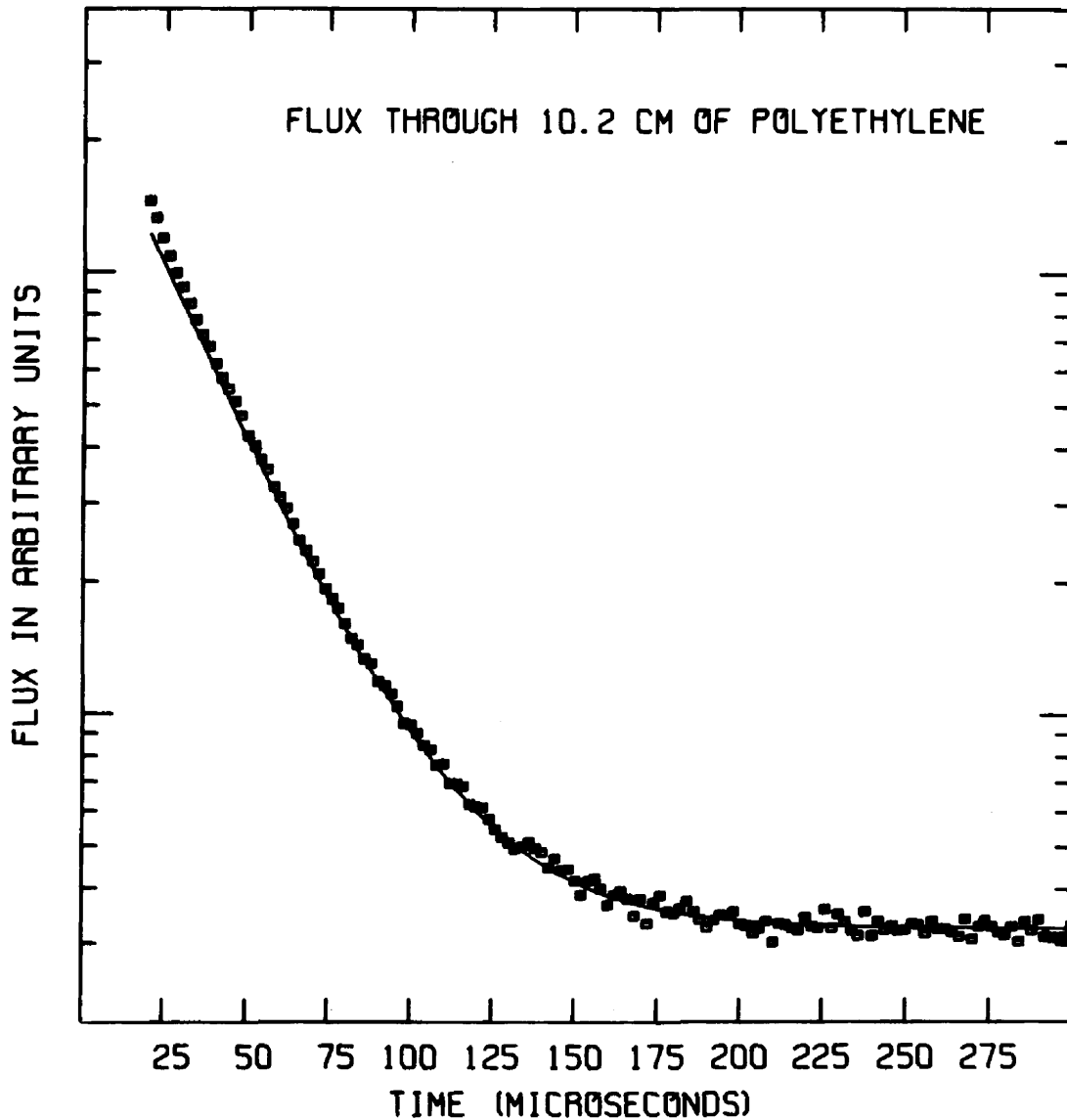


Fig. 4. Flight-time spectrum of "flux" through 10.2 cm of polyethylene which does not pass neutrons below 100 keV (flight times ≥ 35 μ sec). The smooth curve is a visual fit with $A + B \times \exp(-t/18.4 \mu\text{sec})$. The exponential term attenuates with polyethylene as 2.3-MeV gamma radiation.

Using known 18 photon cross sections the strength of the exponential source was corrected to zero polyethylene thickness, normalized to the principal measurement, attenuated for the various filter-sample combinations, and subtracted as background.

The remaining events in the transmission dips of resonances thought to be "black" are not understood in any quantitative fashion; consequently, these events were visually fitted as a function of flight time for each sample-filter combination and subtracted from the spectra as background. To facilitate these subtractions, the functional form of the background was assumed to separate into a flight-time shape, independent of any particular sample-filter combination, and sample and filter scale factors which multiplied this single shape to fit the background for a given sample or a given filter in the beam. By adjusting this shape and these scale factors a quantitative, global, visual fit was obtained which reasonably reproduced the general trend of the remaining background. In particular, this fit required a background shape with both a flight-time independent term and a flight-time exponential decay term with a half-life of 80 μ sec. The scale factors were somewhat proportional to the average transmission of the sample or filter.

In summary, the total background for each time channel and spectrum was written as

$$\text{BGD} = \{7.3 + 13000.0 f_1 f_2 (2)^{-t/18.4} + f_3 f_4 [9.4 + 133.3 (2)^{-t/80.0}]\} b \Delta t \quad (4)$$

where t = channel clock time in μ sec, b = beam burst/ 10^6 , and Δt = channel width in μ sec. The hydrogen capture γ -rays are attenuated with f_1 and f_2 where $f_1 = .930, .787, .364,$ and $.034$ respectively for the 0.076-, 0.254-, 1.080-, and 3.620-cm ^{238}U samples and $f_2 = .69$ for the Al-Mn filter combination. The scale factors for the fitted background are f_3 and f_4 where $f_3 = 0.97, 0.88, 0.60,$ and 0.18 respectively for the ^{238}U samples and $f_4 = .70$ for the Al-Mn filter combination. With an open beam $f_1 = f_2 = f_3 = f_4 = 1.000$.

Table VIII lists the percentage background components of the open beam and the flux through the 3.620-cm sample at three energies where the transmissions through both the ^{238}U and the Al-Mn filters appear constant with energy.

4. Transmission Calculation

Following the background subtraction of Eq. (4), the spectra were divided by their number of beam bursts given in Table VII and various transmissions with statistical errors were calculated. The rapid cycling of the samples and filters into the beam for 20 days assured that the number of beam bursts for each spectrum was proportional to the time-integrated incident flux for each spectrum. Identical (within 0.1%) spectral normalizations are obtained employing the "house monitor" counts per spectrum. The transmission T for each timing channel and ^{238}U sample and its statistical standard deviation ΔT were calculated from the equations,

$$T = \frac{N/B}{N'/B'} \quad (5)$$

and

$$\Delta T = T \sqrt{N \left(\frac{d}{C}\right)^2 + N' \left(\frac{d'}{C'}\right)^2} \quad (5a)$$

where C = sample-in raw events, N = sample-in deadtime-corrected, background-subtracted events, B = sample-in beam burst, and d = sample-in deadtime correction. The primed symbols denote the corresponding sample-out quantities per channel. Corrections were made on these transmissions to account for acrylic coatings on the ^{238}U disk. The largest correction was 1.0% for the 3.62-cm sample at low energies.

From these transmissions cross sections σ per channel and sample thickness and their statistical standard deviations $\Delta\sigma$ were calculated using the equations,

$$\sigma = -(\ln T)/n \quad (6)$$

$$\Delta\sigma = \Delta T/nT \quad (6a)$$

where n is the sample areal density in atoms/barn. These calculated cross sections correspond to real cross sections only in regions of smooth transmission where the resolution broadening has no effect. The resolution broadening acts on the transmission and not on the cross section; consequently, for most energies the calculated cross section of Eq. (6) is not the resolution broadened cross section, but is only proportional to the logarithm of the measured transmission.

Three sets of results were calculated: 1) transmissions through the 0.076-, 0.254-, 1.080-, and 3.620-cm ^{238}U samples with no filters in the beam; 2) transmissions through the four ^{238}U samples with the Al-Mn filter combination in the beam; and 3) transmissions of the Al-Mn filter combination with the open beam spectra and the spectra through the ^{238}U samples which in this case acted as beam filters. The latter two transmission sets were used to help determine the systematic uncertainties in the data; whereas, the former transmission set provided the principal results which are plotted and listed in the next section.

TABLE VIII. Percentage Background Components at Selected Neutron Energies for ORELA 150-m Transmission Measurements

Neutron Energy	^{238}U Sample	Room Background	Hydrogen Capture	Fitted Background
1347.9 eV	open	0.8%	0.0%	2.0%
	3.62 cm	4.8%	0.0%	2.2%
3999.3 eV	open	0.4%	0.1%	2.0%
	3.62 cm	4.2%	0.0%	3.9%
60.60 keV	open	0.1%	2.2%	1.1%
	3.62 cm	0.9%	0.8%	2.0%

IV. RESULTS AND DISCUSSION

1. The Transmissions

The transmissions from 1.0 to 100.0 keV through two of the four ^{238}U samples are histogram plotted in Figs. 5 to 16. For ^{238}U the resonance radiation widths are near 0.023 eV and approximately constant with energy, the average s-wave and p-wave neutron widths increase with energy approximately as $0.002 \sqrt{E}$ eV and $1.0 \times 10^{-9} E^{3/2}$ eV, respectively, and the Doppler broadening FWHM increases as $0.035 \sqrt{E}$ eV where E is the neutron energy also in eV. Consequently almost all ^{238}U resonances have natural widths much smaller than their Doppler widths and the Doppler broadening determines the possible observable widths of the transmission structure.

Figures 5, 6, and 7 show the 0.254- and 3.620-cm transmissions from 1.0 to 4.0 keV plotted in 0.5-keV intervals. Our previous 40 m data were least-squares shape fitted up to 1.087 keV, so a similar analysis of the new transmissions over the energy range of Figs. 5, 6, and 7 will provide ORELA ^{238}U neutron widths for the entire resolved resonance region of the ENDF evaluation. Below 4.0 keV the energy resolution is less than or roughly equal to the Doppler width.

Figures 8 and 9 show transmissions plotted in 1.0-keV intervals through the 0.254- and 3.620-cm samples from 4.0 to 8.0 keV which is an energy range equal to and immediately following the resolved resonance region. From 4.0 to 8.0 keV our energy resolution is roughly equal to or greater than the Doppler width. Carraro and Kolar² analyzed their transmissions to 5.7 keV, whereas Rahn *et al.*,³ Nakajima *et al.*,⁴ and Poortmans *et al.*⁵ report neutron widths to around 4.5 keV. Our transmissions should be analyzable up to 6.0 keV and perhaps up to 8.0 keV. At 8.0 keV the Doppler width is one-eighth of the average s-wave level spacing of 24 eV.

Figures 10 through 14 show transmissions in the unresolved resonance region where individual resonance parameters cannot be extracted from the experimental data, but still drastically affect the cross sections. In particular, Figs. 10, 11, and 12 show transmissions through the 0.254- and

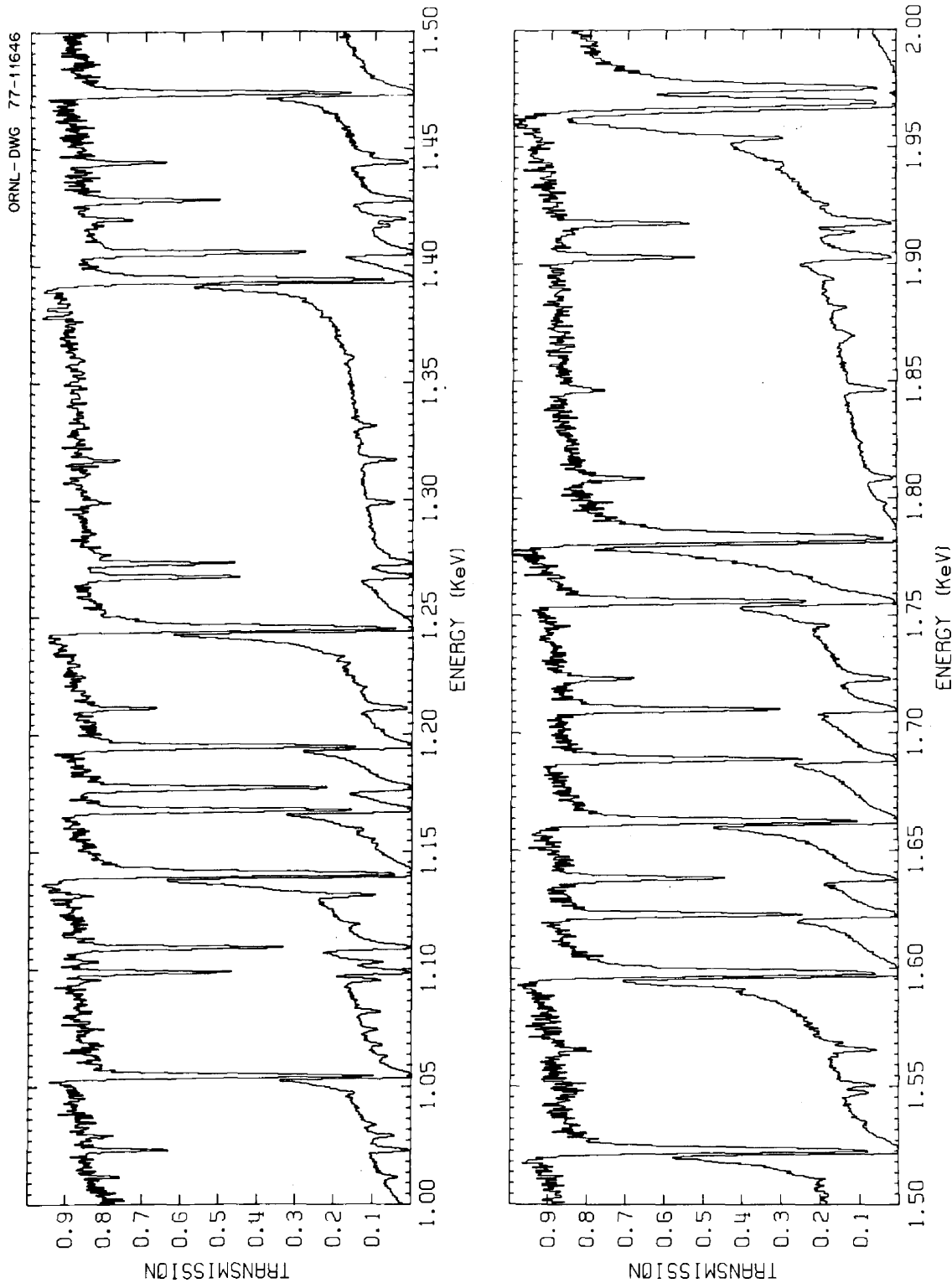


Fig. 5. Measured neutron transmissions through 0.254- and 3.620-cm-thick ^{238}U samples.

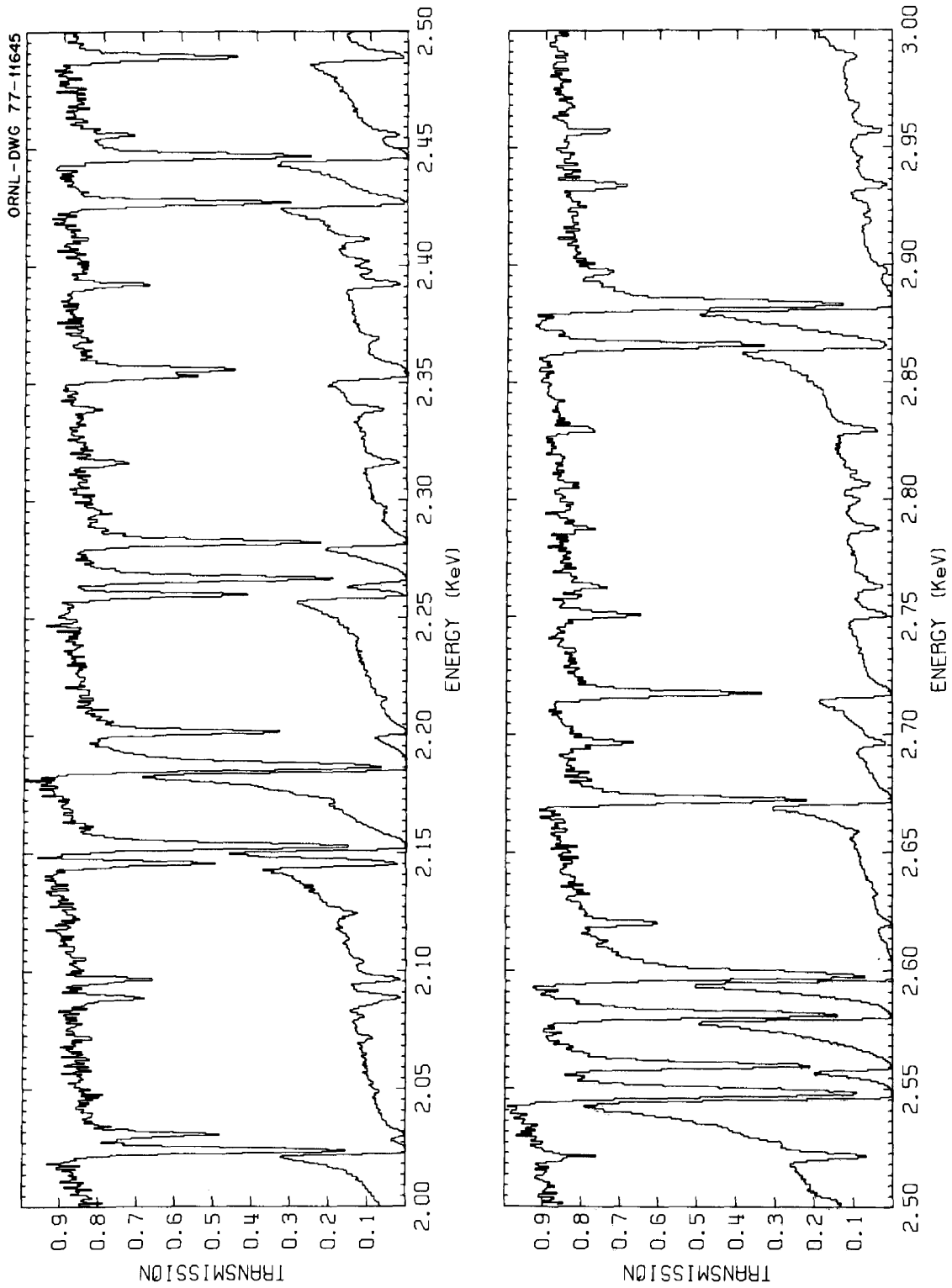


Fig. 6. Measured neutron transmissions through 0.254- and 3.620-cm-thick ^{238}U samples.

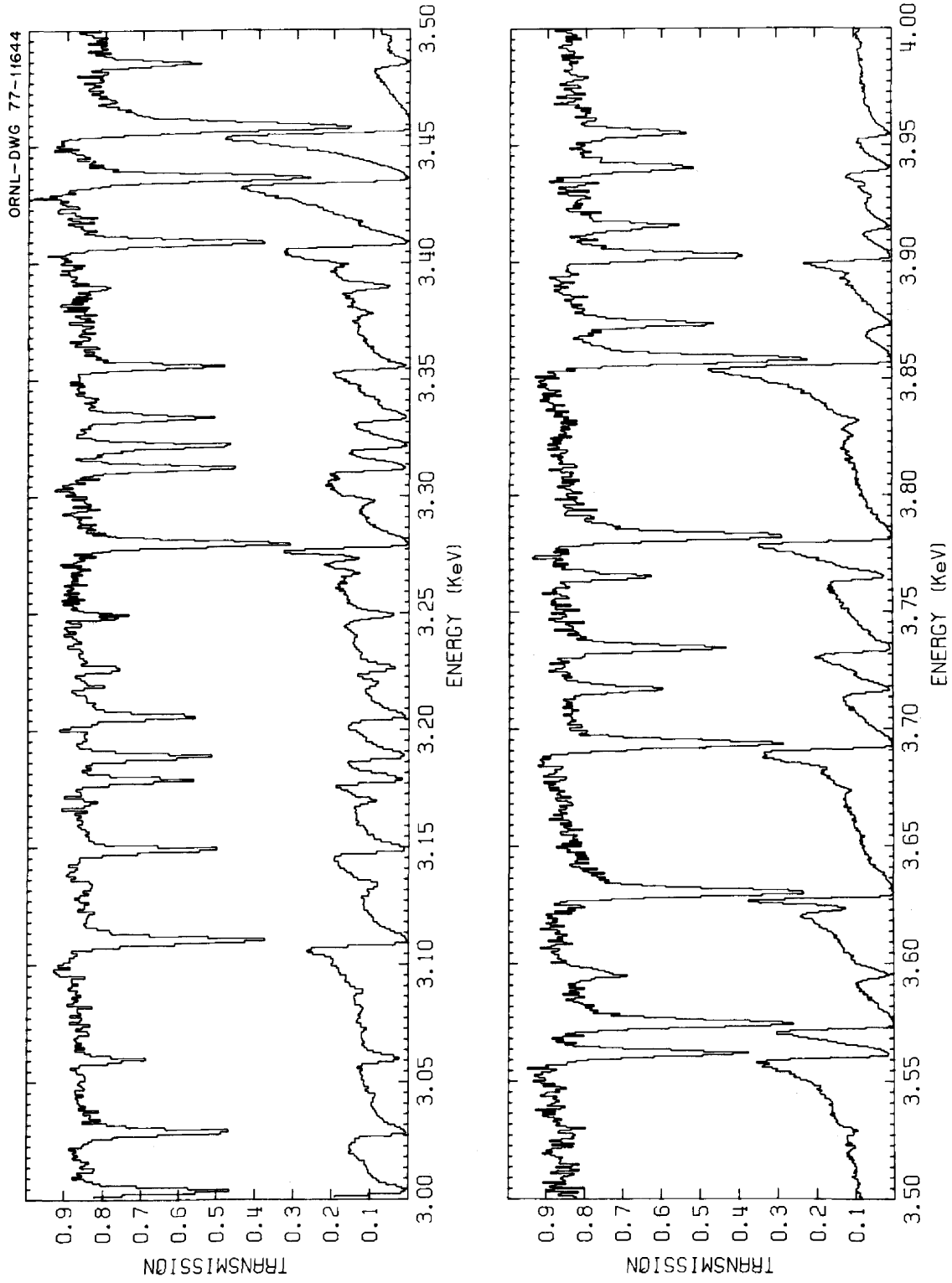


Fig. 7. Measured neutron transmissions through 0.254- and 3.620-cm-thick ^{238}U samples.

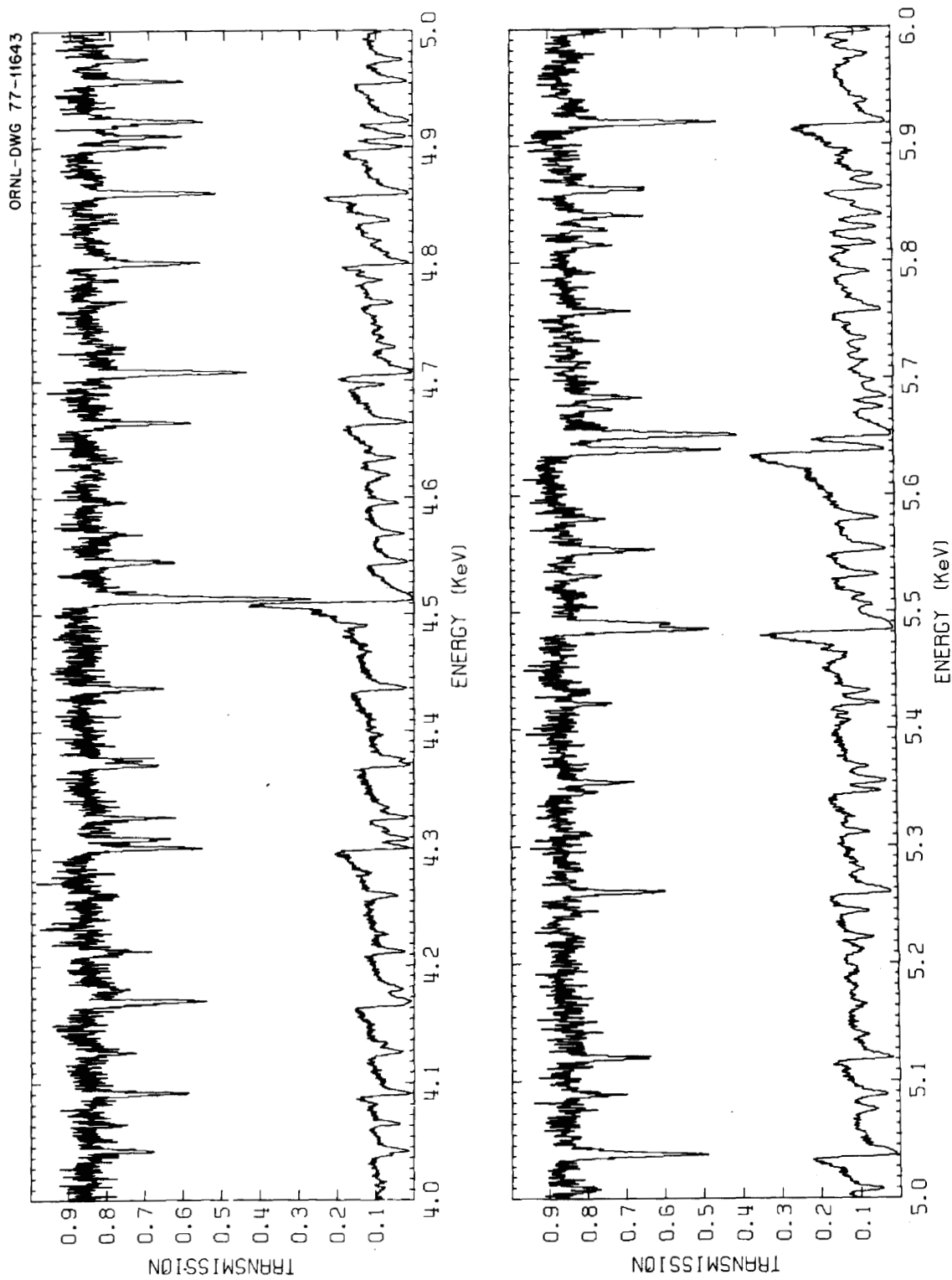


Fig. 8. Measured neutron transmissions through 0.254- and 3.620-cm-thick ²³⁸U samples.

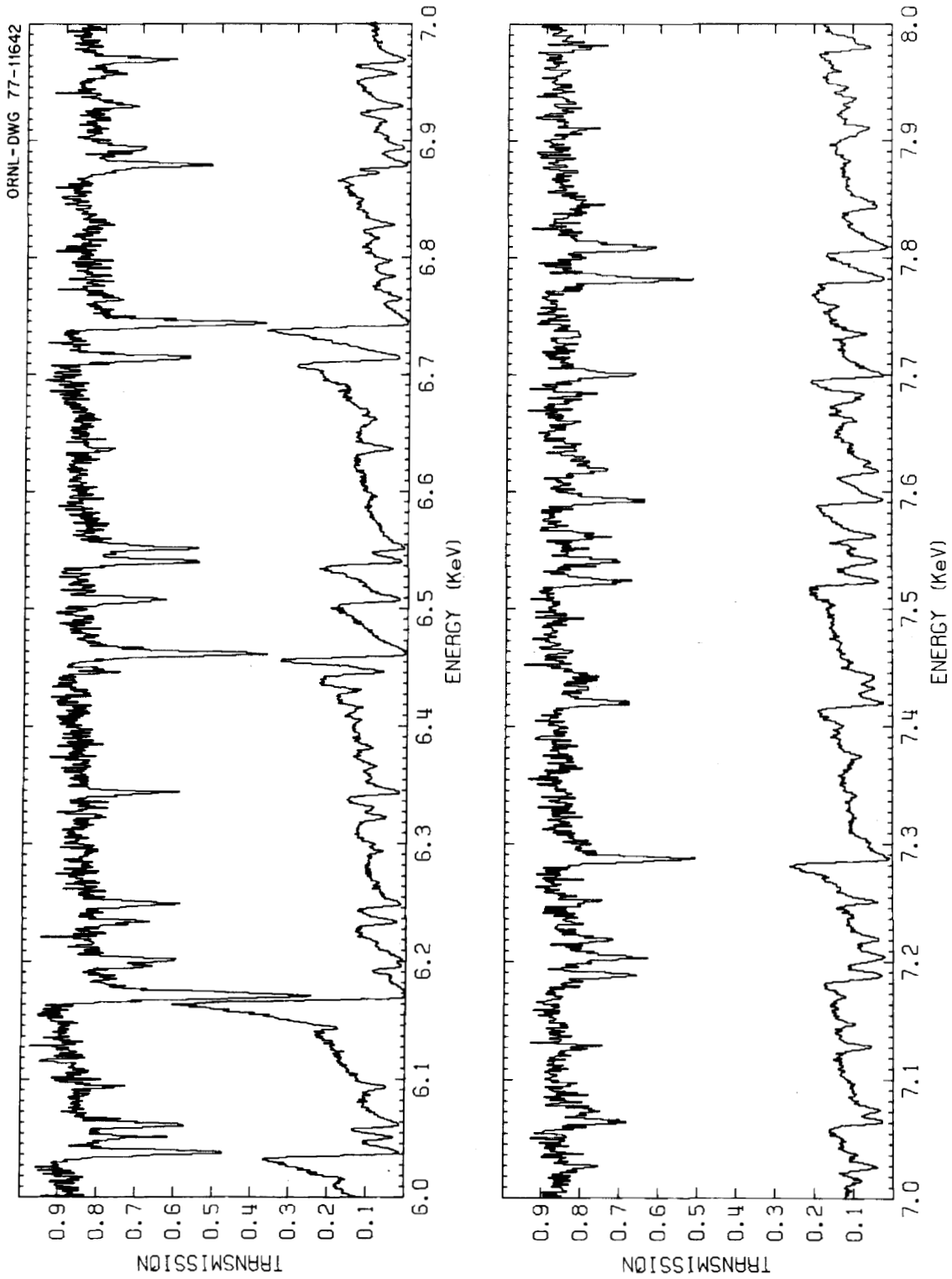


Fig. 9. Measured neutron transmissions through 0.254- and 3.620-cm-thick ²³⁸U samples.

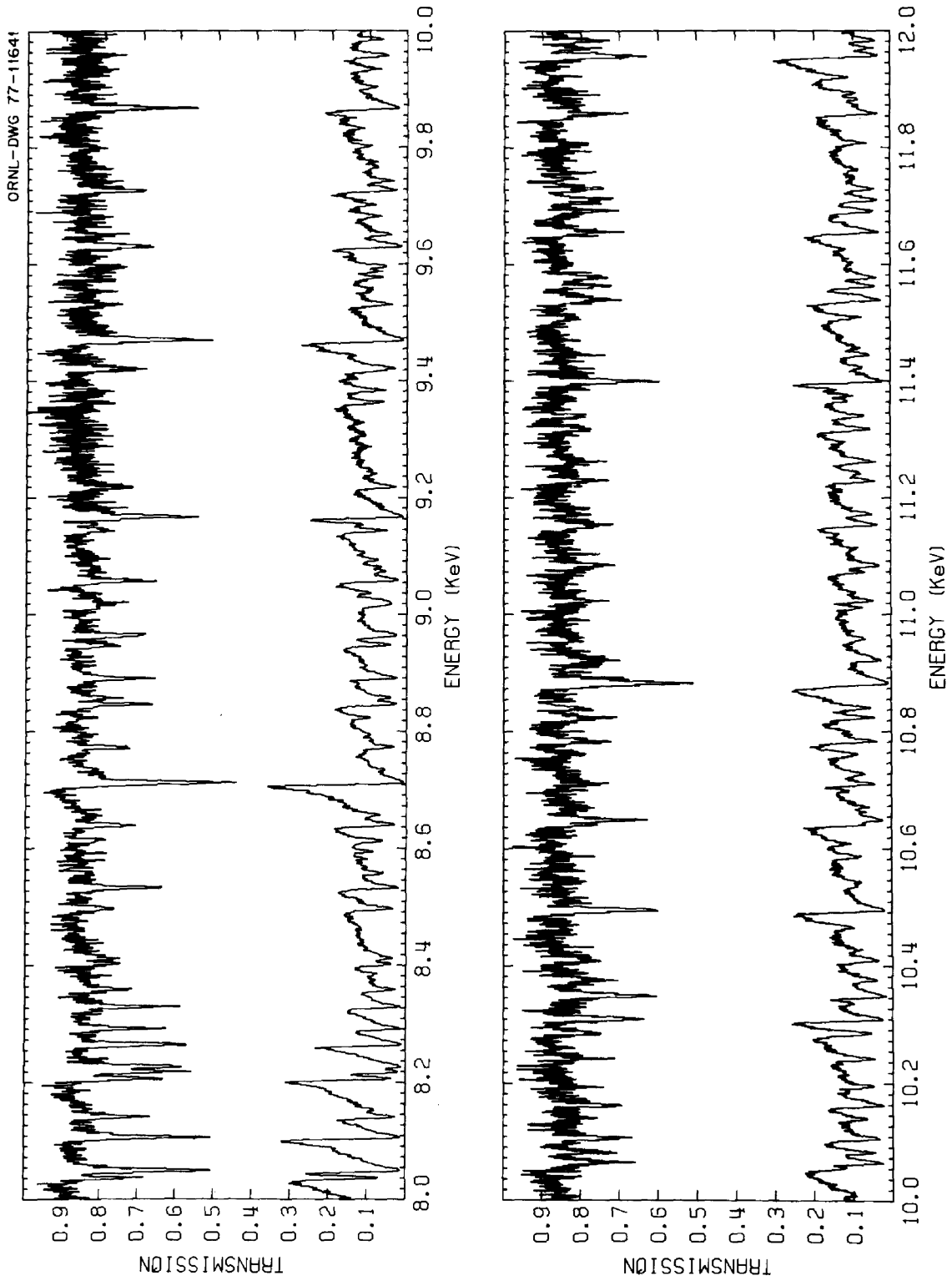


Fig. 10. Measured neutron transmissions through 0.254- and 3.620-cm-thick ^{238}U samples.

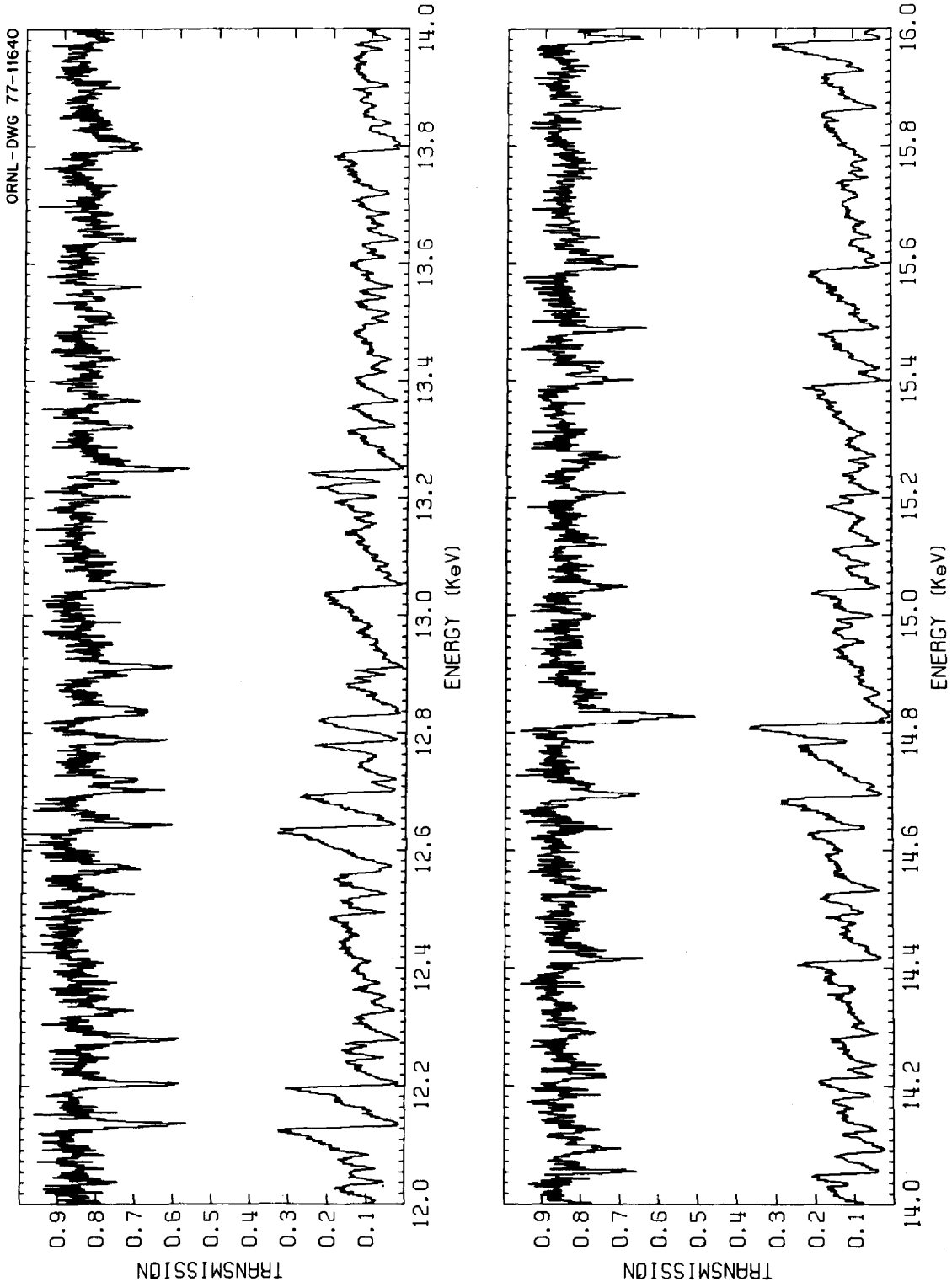


Fig. 11. Measured neutron transmissions through 0.254- and 3.620-cm-thick ^{238}U samples.

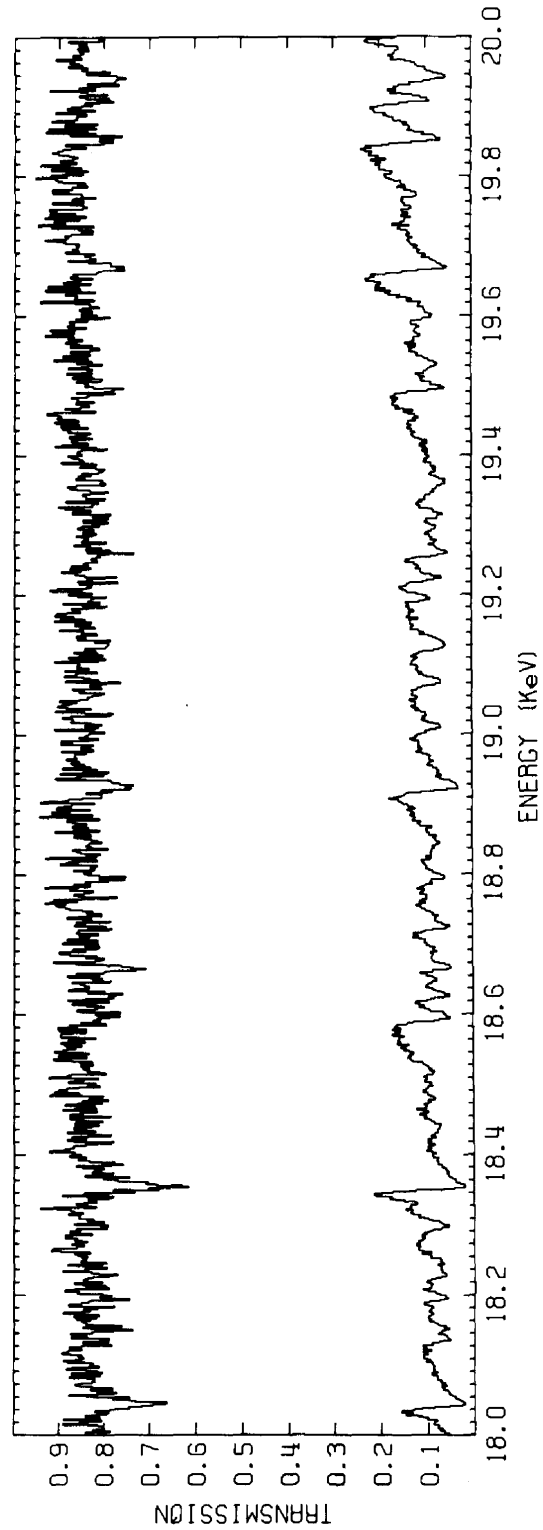
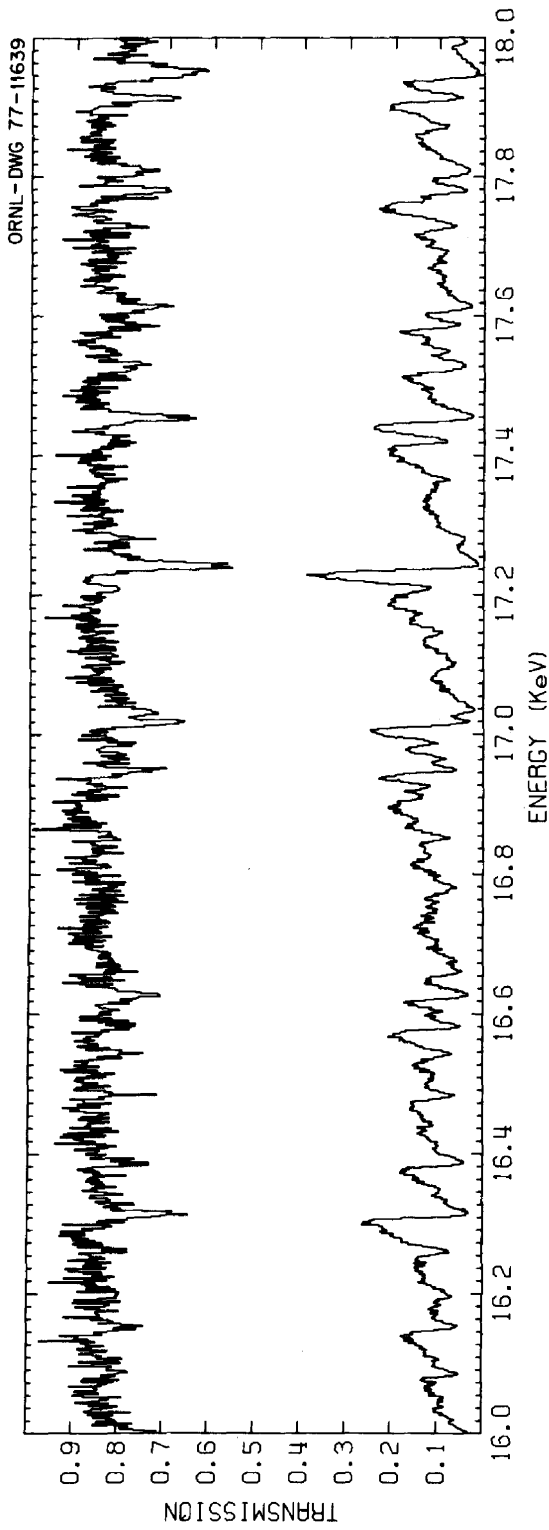


Fig. 12. Measured neutron transmissions through 0.254- and 3.620-cm-thick ^{238}U samples.

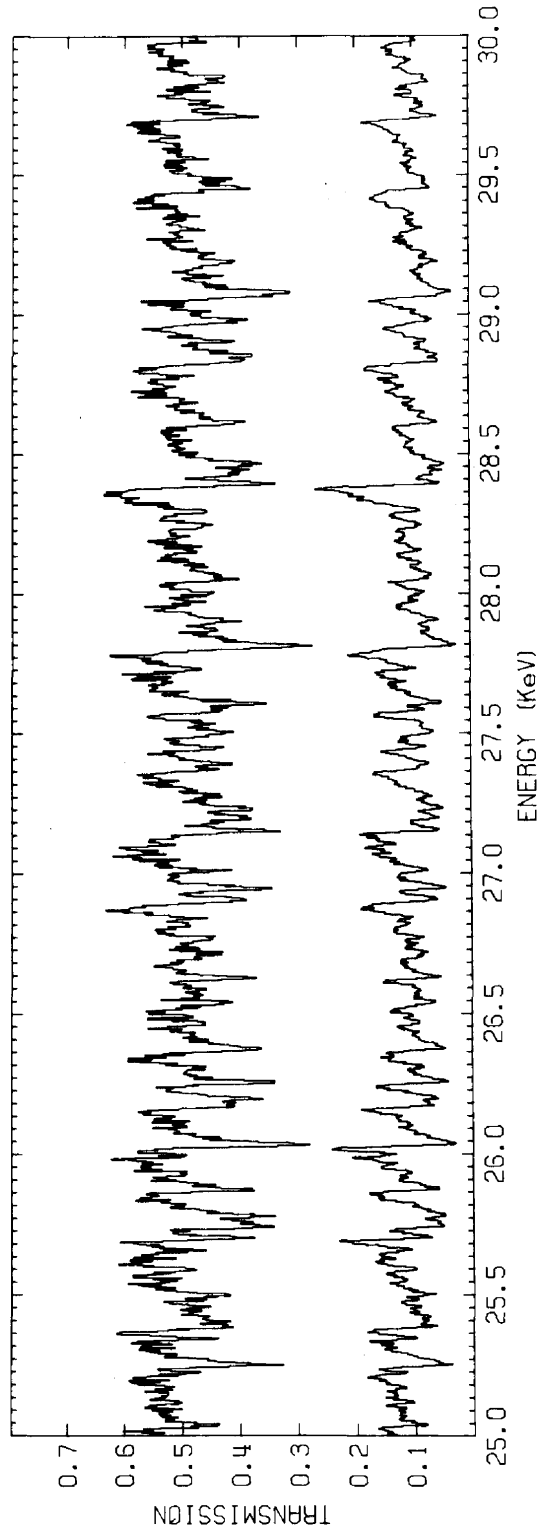
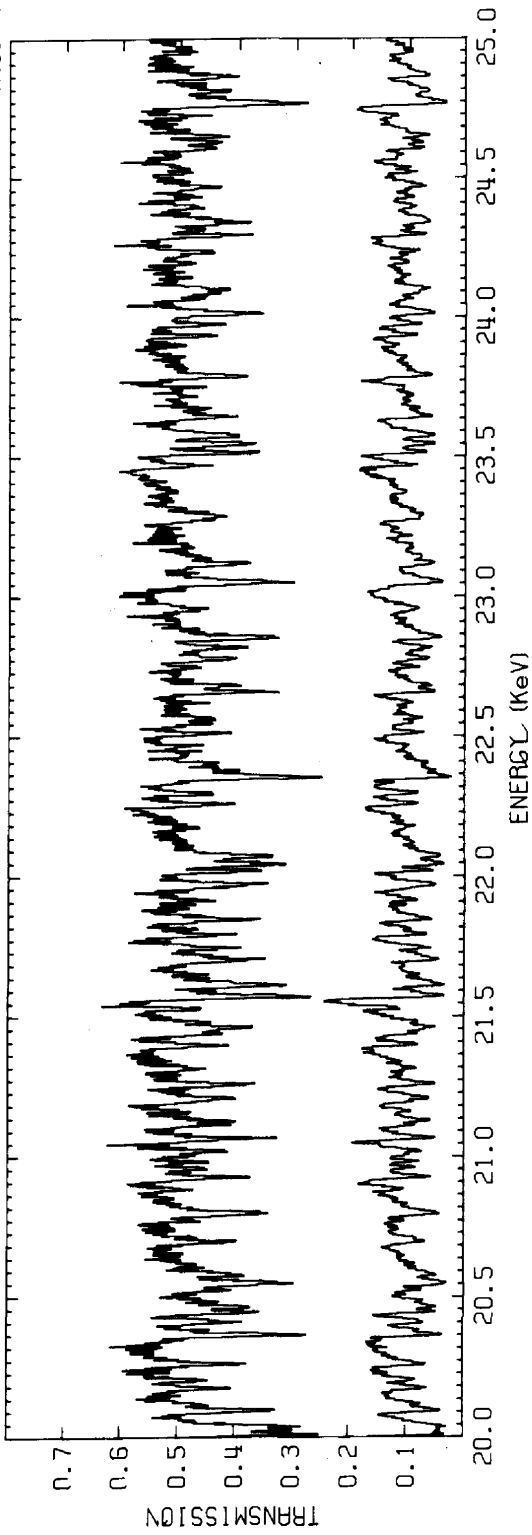


Fig. 13. Measured neutron transmission spectra through 1.080- and 3.620-cm-thick ^{238}U samples.

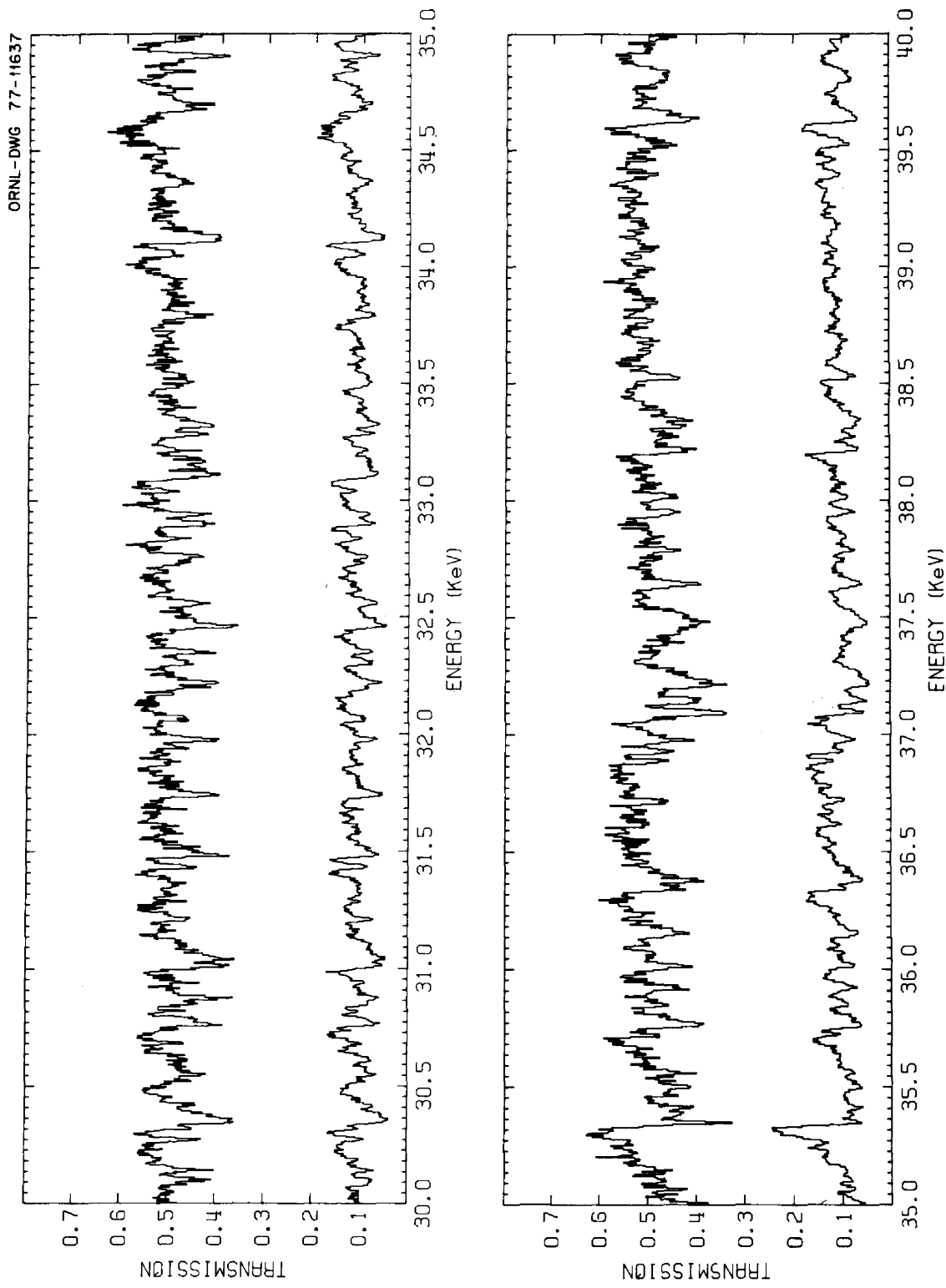


Fig. 14. Measured neutron transmission spectra through 1.080- and 3.620-cm-thick ^{238}U samples.

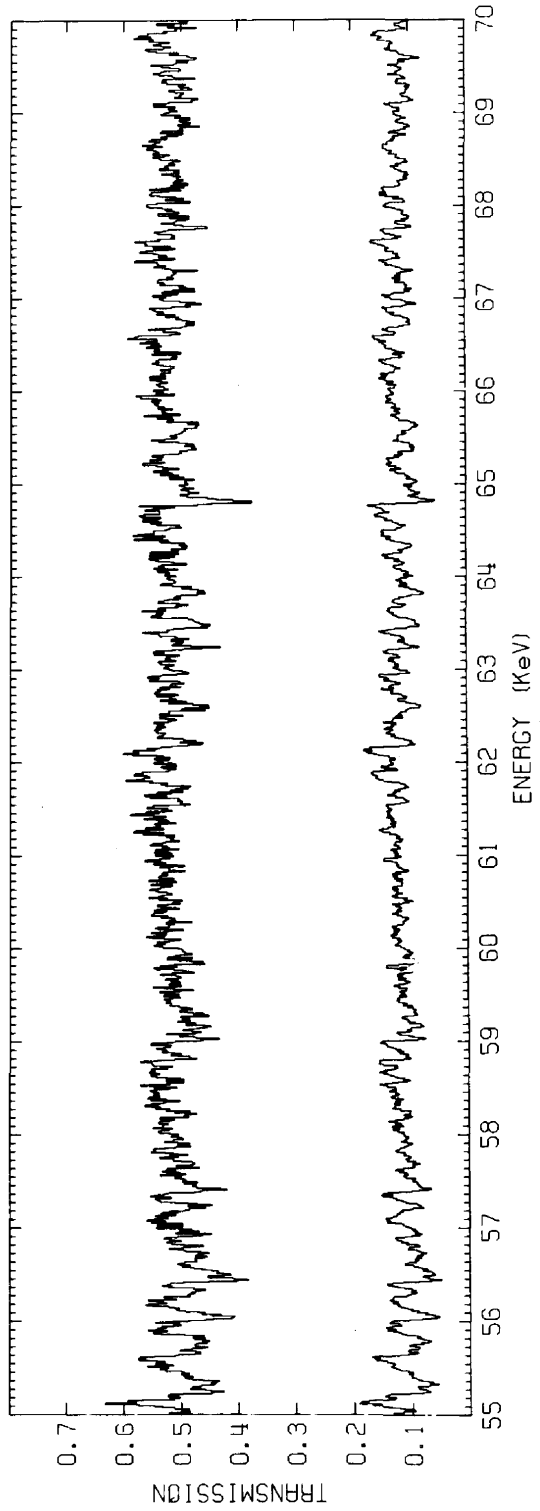
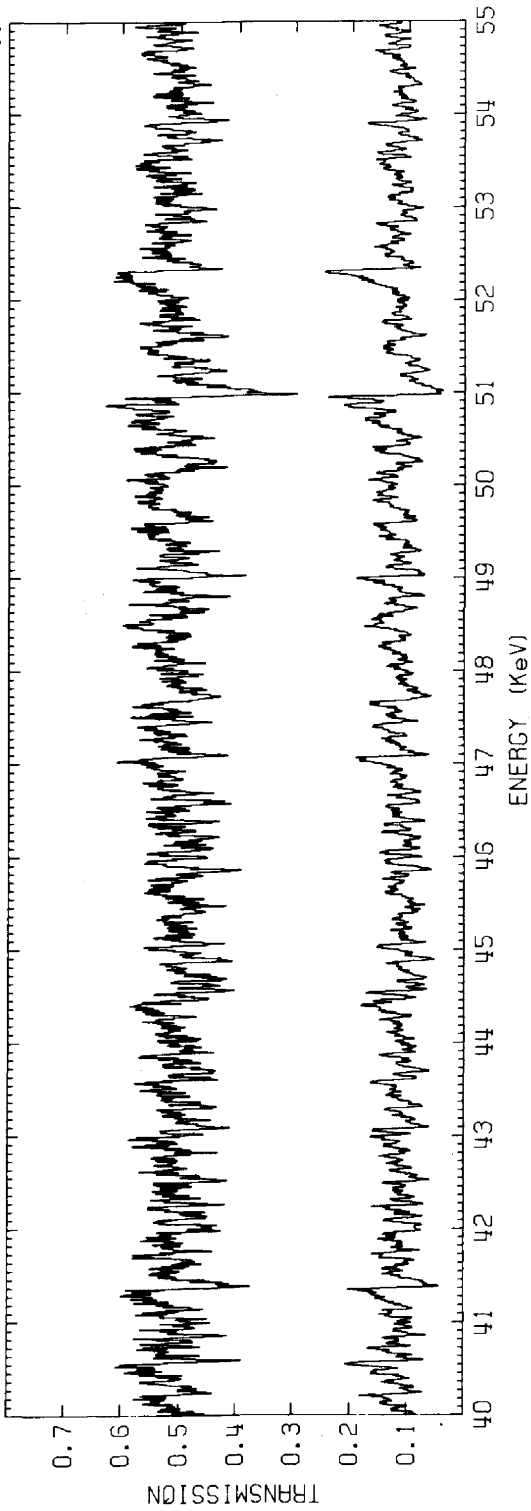
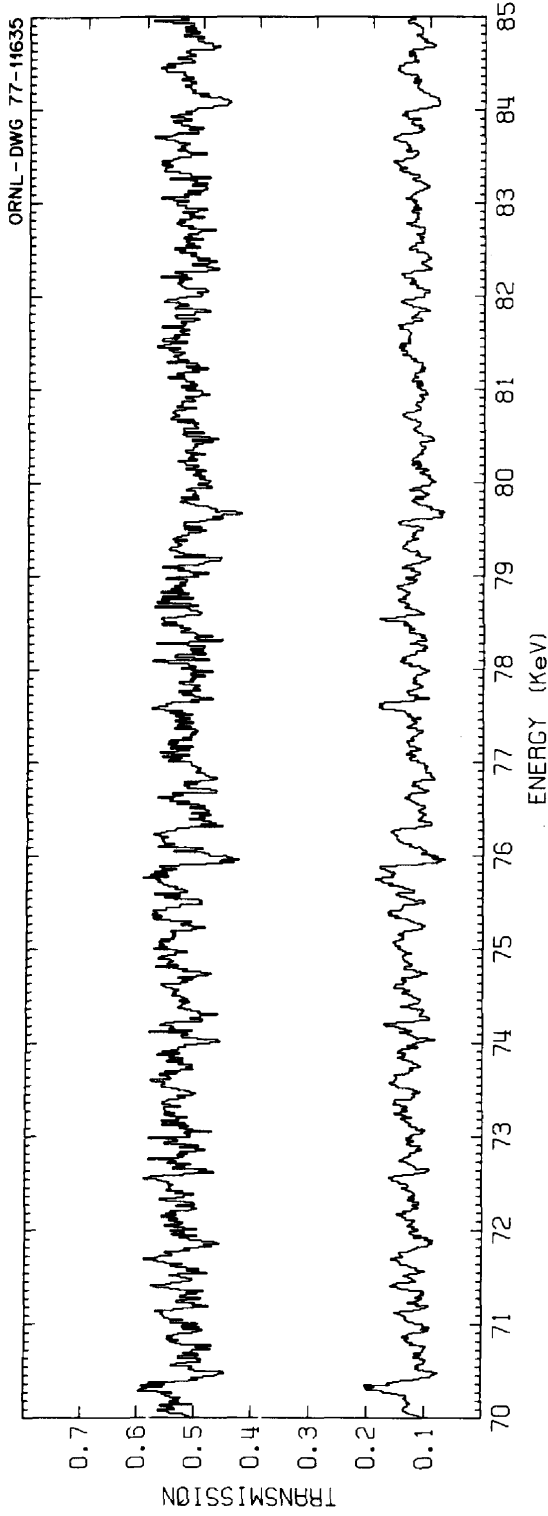


Fig. 15. Measured neutron transmission spectra through 1.080- and 3.620-cm-thick ²³⁸U samples.



33

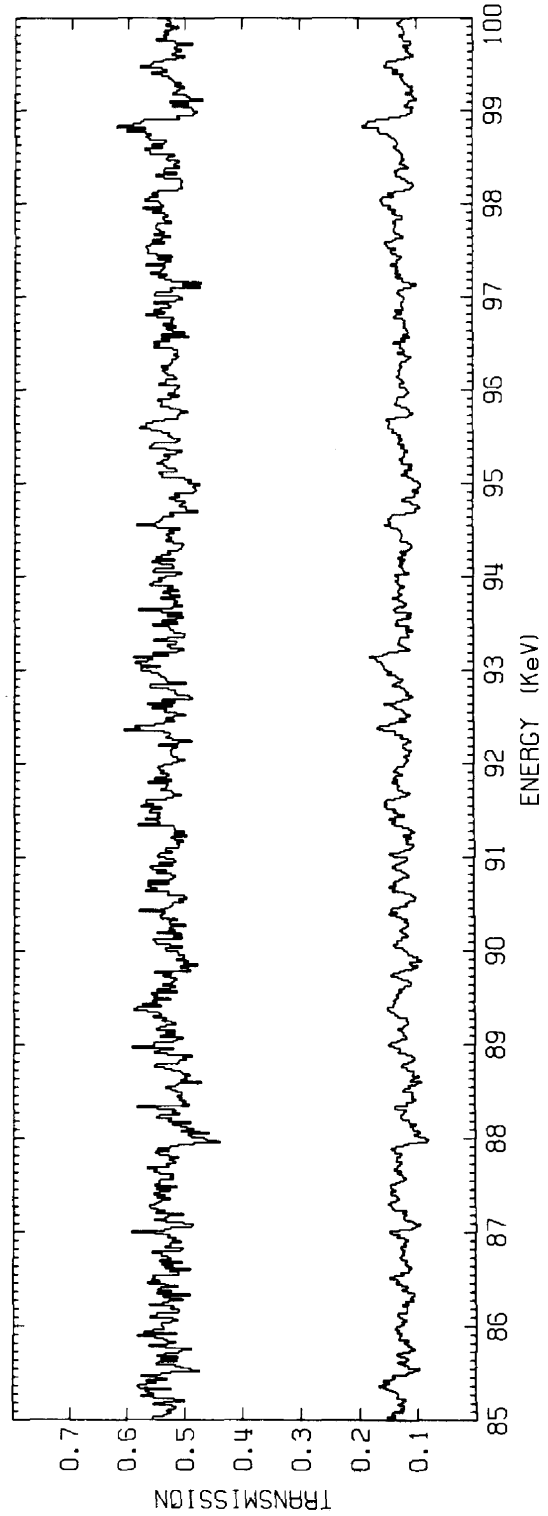


Fig. 16. Measured neutron transmission spectra through 1.080- and 3.620-cm-thick ^{238}U samples.

3.620-cm samples from 8.0 to 20.0 keV plotted in 2.0-keV intervals, and Figs. 13 and 14 show transmissions through the 1.080- and 3.620-cm samples from 20.0 to 4.0 keV plotted in 5.0-keV intervals. Over these energies the cross sections obtained from applying Eq. (6) directly to the measured transmissions is very sample thickness dependent.

To first order the resolution broadening of the transmission spectra, ignoring the small smearing from finite channels, can be approximated by a Gaussian function whose width R , FWHM in eV, can be written as

$$R = E\sqrt{\alpha+\beta E}$$

with

$$\alpha = (2\Delta L/L)^2$$

and

$$\beta = (2\Delta t/72.3L)^2$$

where ΔL is the equivalent-distance moderation width in mm, Δt is the electron beam burst FWHM of 12 nsec, L is the flight path in mm, and E is the neutron energy in eV. Values of ΔL ranging from 25 mm,⁹ which is the theoretical estimate from moderation only, to 50 mm,¹⁹ which probably includes some detector effects, have been used at ORELA. Assuming $\Delta L = 33$ mm the resolution FWHM at 40.0 keV is 24 eV with equal contributions from the equivalent-distance moderation width and the beam burst width.

Figures 15 and 16 show transmissions through the 1.080- and 3.620-cm sample from 40.0 to 100.0 keV plotted in 15-keV intervals. The unresolved resonance region of ENDF/B-IV extends to 45 keV above which a smooth cross section is assumed. Our transmission through the thickest sample shows considerable structure which probably arises from the largest s-wave resonances or clusters of large s-wave resonances. At 100.0 keV our resolution width is in the order of 100 eV, the Doppler width is 11 eV, and extrapolating from low energies the average s-wave and p-wave level spacings are about 25 eV and 8 eV, respectively. The transmissions from 0.880 to 100.0 keV through all four sample thicknesses are listed in the Appendix.

At sufficiently high neutron energies the Doppler broadened total cross section should be smooth; consequently, the resolution function has no effect and the true cross section should be directly attainable with Eq. (6) from any thick-sample transmission. Figure 17 shows histogram plots from 10 to 100 keV of "cross sections" from our two thick-sample transmissions. In particular, the upper and lower histograms are from the application of Eq. (6) to the 1.080- and 3.620-cm transmission, respectively, after averaging over time intervals corresponding to 5 keV energy intervals. Assuming an open-beam spectrum smooth with energy, these total "cross sections" are those which would be obtained from a very low resolution transmission measurement. The two "cross sections" converge toward common values with increasing energy. At 100 keV they differ by about 3%. Some of this 3% difference could be explained by systematic uncertainties in the measured transmissions which are discussed in the next subsection.

2. Discussion of Uncertainties

Both statistical and systematic uncertainties exist in the measured transmissions. The statistical uncertainties have been propagated with Eq. (5a) from the measured events per channel to the transmissions and are the errors listed in the Appendix. The systematic uncertainties arise from the deadtime correction, background subtraction, sample thickness and composition, spectral normalizations, and possible confusion in the understanding and operation of the experimental apparatus. Errors from the deadtime, sample, and normalizations are believed to be small. The other systematic errors are very difficult to assess.

Perhaps the best estimate of the total systematic uncertainty of the data can be obtained from internal consistency which is illustrated in Table IX where cross sections from the four ^{238}U transmissions both with and without the Al-Mn filter and the corresponding transmissions through the Al-Mn filter are listed. These data are averaged over the column-one energy intervals in which the transmissions through both the ^{238}U and the Al-Mn appeared particularly constant and smooth with energy. The errors

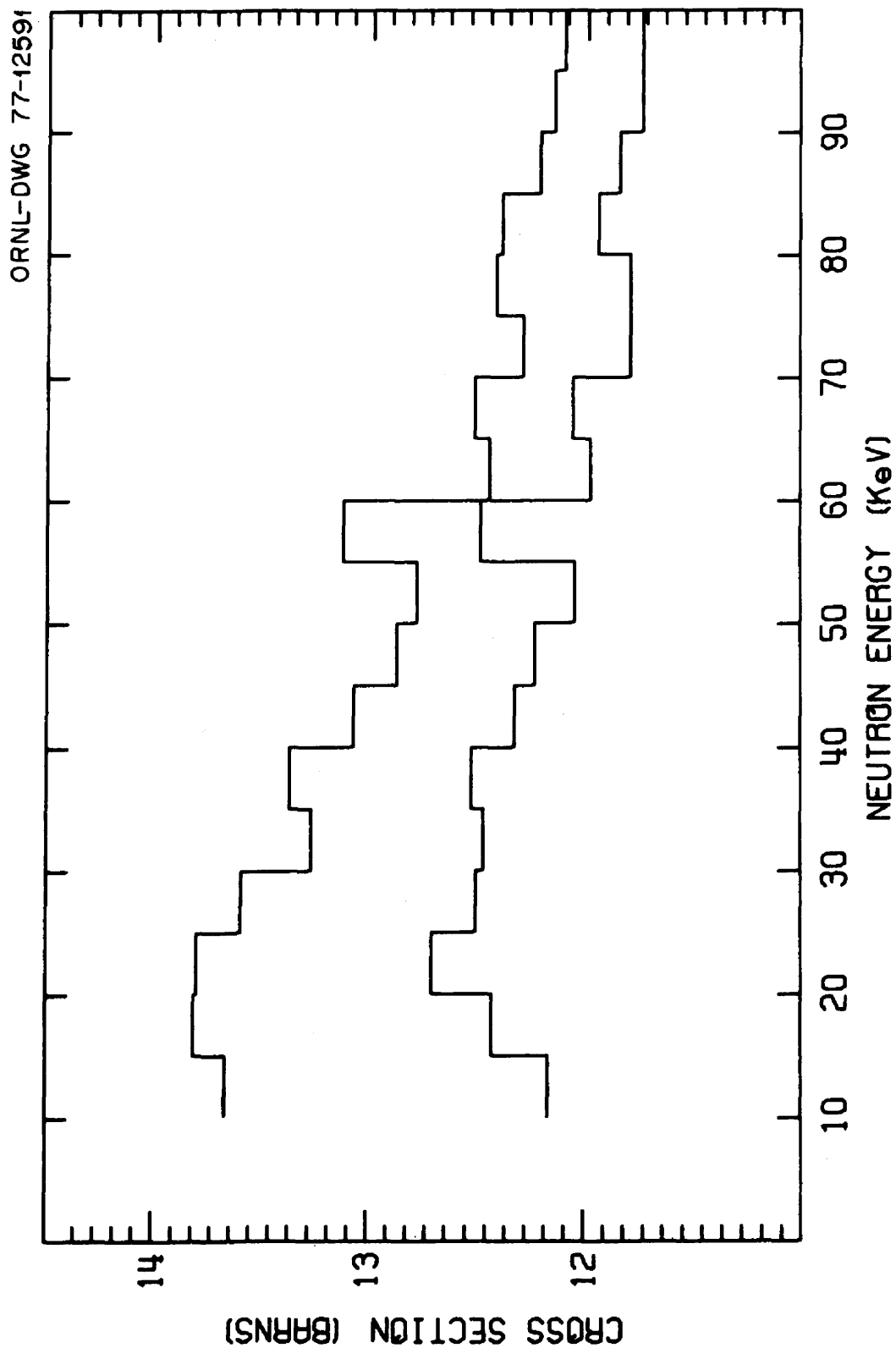


Fig. 17. Total neutron "cross sections" obtained from the 1.080-cm (upper) and 3.620-cm (lower) transmissions averaged over time intervals corresponding to 5.0-keV energy intervals. The statistical uncertainties are negligible and the systematic uncertainties are ± 0.3 and ± 0.1 barns for the upper and lower histograms respectively.

TABLE IX. Comparison of Cross Sections in Barns and Transmissions with Statistical Uncertainties from the Ten Measured Flight-Time Spectra

Energy Interval	Sample (cm)	σ of ^{238}U without Al-Mn	σ of ^{238}U with Al-Mn	T of Al-Mn with ^{238}U
1334.1 to 1355.1 eV	3.620	$10.53 \pm .02$	$10.49 \pm .05$	$.779 \pm .006$
	1.080	$10.61 \pm .06$	$10.61 \pm .11$	$.771 \pm .004$
	0.254	$10.5 \pm .3$	$10.5 \pm .5$	$.771 \pm .004$
	0.076	$9.7 \pm .8$	9.7 ± 1.6	$.772 \pm .004$
	open			$.772 \pm .004$
3981.6 to 4017.6 eV	3.620	$13.91 \pm .04$	$14.00 \pm .07$	$.769 \pm .010$
	1.080	$14.04 \pm .08$	$14.17 \pm .14$	$.771 \pm .005$
	0.254	$13.3 \pm .3$	$14.4 \pm .6$	$.765 \pm .005$
	0.076	13.0 ± 1.0	14.6 ± 2.0	$.772 \pm .005$
	open			$.776 \pm .005$
60.209 to 61.005 keV	3.620	$11.93 \pm .03$	$11.98 \pm .05$	$.762 \pm .007$
	1.080	$11.94 \pm .06$	$11.92 \pm .12$	$.766 \pm .004$
	0.254	$11.2 \pm .2$	$11.8 \pm .5$	$.760 \pm .004$
	0.076	$11.1 \pm .9$	$10.0 \pm .6$	$.769 \pm .004$
	open			$.766 \pm .004$

are statistical only. These data and similar comparisons in other energy intervals indicate that at all energies below 100 keV the various transmissions appear to be consistent to about 1.5% of the average or potential scattering values. Consequently, total systematic uncertainties of ± 0.014 , ± 0.013 , ± 0.008 , and ± 0.002 are assigned to the 0.076-, 0.254-, 1.080-, and 3.620-cm transmissions respectively. These transmission uncertainties correspond to potential scattering or average cross section uncertainties of ± 4.0 , ± 1.2 , ± 0.3 , ± 0.1 barns respectively.

In addition, smooth cross sections from the present 150 m measurements can be compared with those from the previous 40 m measurements⁶ in their region of overlap. This is done in Table X for the 1345- and 4000-eV intervals where the errors are statistical standard deviations only. The agreement between the two measurements through the thickest sample is excellent. Moreover, the 40 m measurements contained a 2 to 3% systematic discrepancy between smooth cross sections from the 3.620- and 1.080-cm samples. In the present measurement this cross section difference between the two samples has been reduced to 1.0%.

TABLE X. Comparison Between Cross Sections from the Present 150-m Measurements and the Previous 40-m Measurements

Energy Interval	Sample Thickness	Cross Section	
		150 m	40 m
1334.1 to 1355.1 eV	3.620 cm	$10.53 \pm .02$ b	$10.51 \pm .03$ b
	1.080 cm	$10.61 \pm .06$ b	$10.69 \pm .15$ b
3981.6 to 4017.6 eV	3.620 cm	$13.91 \pm .04$ b	$13.89 \pm .11$ b
	1.080 cm	$14.04 \pm .08$ b	$14.25 \pm .30$ b

V. ACKNOWLEDGMENTS

The authors are indebted to the entire ORELA staff for the excellent linac operation. J. G. Craven wrote the computer program for data acquisition. Appreciation is expressed to L. O. Love and H. R. Gwinn for performing the isotope separation and to G. Mitchell (Y-12) and E. H. Kobisk for reducing the material to metal and machining the finished samples. The authors gratefully acknowledge many helpful discussions with and advice from J. A. Harvey and R. L. Macklin. The Physics Division is thanked for the loan of the Li-glass detector.

REFERENCES

1. J. B. Garg, J. Rainwater, J. S. Petersen, and W. W. Havens, Jr., *Phys. Rev.* 134, B985 (1964).
2. G. Carraro and W. Kolar, in *Proc. Int. Conf. Nuclear Data for Reactors, Helsinki, IAEA-CN-26/T16, I, 403*, International Atomic Energy Agency, Vienna (1970).
3. F. Rahn, H. S. Camarda, G. Hacken, W. W. Havens, Jr., H. I. Liou, J. Rainwater, M. Slagowitz, and S. Wynchank, *Phys. Rev. C* 6, 1854 (1972).
4. Y. Nakajima, A. Asami, M. Mizumoto, T. Fuketa, and H. Takekoshi, *Proc. Conf. Neutron Cross Sections and Technology*, Washington, DC, NBS 425, p. 738, National Bureau of Standards (1975).
5. F. Poortmans, L. Mewissen, G. Rohr, H. Weigmann, and G. Vanpraet, *Proc. Int. Conf. on Interactions of Neutrons and Nuclei*, Lowell, Mass., Conf-760715, p. 1264 (1976); F. Poortmans, private communication (1977).
6. D. K. Olsen, G. de Saussure, R. B. Perez, E. G. Silver, R. W. Ingle, and H. Weaver, "Measurement of Neutron Transmissions from 0.52 eV to 4.0 keV Through Seven Samples of ^{238}U at 40 m," ORNL/TM-5256, Oak Ridge National Laboratory (1976); D. K. Olsen, G. de Saussure, R. B. Perez, E. G. Silver, F. C. Difilippo, R. W. Ingle, and H. Weaver, *Nucl. Sci. Eng.* 62, 479 (1977).
7. Conclusions and Recommendations of Proc. Specialists Meeting on "Resonance Parameters of Fertile Nuclei and ^{239}Pu ," Saclay, May 1974, edited by P. Ribon, NEANDC(%) 163U, p. 6.
8. D. I. Garber and R. R. Kinsey, BNL 325, Third Edition, Vol. II, p. 455 (1976).
9. R. L. Macklin, *Nucl. Instrum. Methods* 91, 79 (1971).
10. E. G. Silver, R. W. Ingle, G. de Saussure, R. B. Perez, H. Weaver, and R. J. Robson, "Neutron Physics Division Annual Progress Report for Period Ending May 31, 1972," ORNL-4800, p. 8 (1972).
11. Charles Stanley, Engineering Division, ORNL, private communication (1977).
12. KGLL, Koch-Light Lab. Ltd., Scintillation Division, Colnbrook, Buckinghamshire, England.
13. J. H. Todd, "Instrument and Controls Division Annual Progress Report for Period Ending September 1, 1970," ORNL-4620, p. 36, Oak Ridge National Laboratory (1970).

14. J. H. Todd, "Instrumentation and Controls Division Annual Progress Report for Period Ending September 1, 1968," ORNL-4335, p. 17, Oak Ridge National Laboratory (1969).
15. Strouse, Inc., Morristown, Pennsylvania 19404; No. 8010-515-2487 lacquer enamel; Fed. Spec. TT-L-50e, Type II clear; Contract No. GS-00S-89623; 9.1% hydrogen content by weight.
16. D. K. Olsen, G. de Saussure, R. B. Perez, F. C. Difilippo, and R. W. Ingle, "Note on $^{238}\text{U}+n$ Resolved Resonance Energies," accepted for publication in Nuclear Science and Engineering.
17. J. A. Harvey, C. H. Johnson, W. E. Kinney, and R. L. Macklin, ORNL, private communication (1976).
18. E. Storm and H. I. Israel, Nuclear Data Tables 7, 565 (1970).
19. D. C. Larson, C. H. Johnson, J. A. Harvey, and N. W. Hill, "Measurement of the Neutron Total Cross Section of Fluorine from 5 eV to 20 MeV," ORNL/TM-5612 (1976).

APPENDIX

This appendix lists the four measured transmissions through the 0.00376-, 0.01239-, 0.05208-, and 0.17536-atom/barn ^{238}U samples for 39,239 energies from 99985.11 to 880.13 eV. The following typed page is the first page of this listing. These and the remaining 676 pages of transmissions are given on the three microfiche sheets contained in the envelope attached to the inside back cover of this report. Each line of the appendix gives the energy of the channel center followed by the four transmission values where each transmission is immediately followed by its statistical standard deviation. These errors are statistical only and do not contain the systematic uncertainties which have been discussed in Section IV-2. The listed transmissions have been corrected for the acrylic coatings on the ^{238}U disk. These data have been transmitted to the National Nuclear Data Center at Brookhaven National Laboratory.

ENERGY	0.00376A/B		0.01239A/B		0.05208A/B		0.17536A/B	
99985.11	0.987	0.025	0.863	0.022	0.532	0.014	0.1230	0.0043
99962.60	0.938	0.023	0.839	0.021	0.527	0.014	0.1261	0.0043
99940.11	0.968	0.024	0.862	0.021	0.525	0.014	0.1323	0.0045
99917.62	0.962	0.024	0.850	0.021	0.534	0.014	0.1293	0.0044
99895.14	0.913	0.023	0.843	0.021	0.511	0.013	0.1232	0.0042
99872.66	0.991	0.024	0.861	0.021	0.526	0.014	0.1209	0.0042
99850.20	0.946	0.024	0.866	0.022	0.537	0.014	0.1200	0.0042
99827.74	0.958	0.024	0.875	0.022	0.530	0.014	0.1196	0.0042
99805.29	0.981	0.024	0.857	0.021	0.539	0.014	0.1285	0.0044
99782.84	0.994	0.025	0.889	0.022	0.533	0.014	0.1220	0.0043
99760.41	0.953	0.024	0.893	0.022	0.552	0.014	0.1218	0.0043
99737.98	0.948	0.024	0.844	0.021	0.517	0.014	0.1098	0.0040
99715.56	0.931	0.023	0.819	0.020	0.487	0.013	0.1092	0.0040
99693.14	0.974	0.024	0.881	0.022	0.515	0.014	0.1222	0.0043
99670.74	0.953	0.024	0.862	0.022	0.520	0.014	0.1136	0.0041
99648.34	0.963	0.024	0.885	0.022	0.507	0.013	0.1187	0.0042
99625.95	0.963	0.024	0.860	0.022	0.517	0.014	0.1133	0.0041
99603.57	0.956	0.024	0.850	0.021	0.525	0.014	0.1106	0.0041
99581.19	0.957	0.024	0.860	0.021	0.499	0.013	0.1046	0.0039
99558.82	0.960	0.024	0.833	0.021	0.517	0.014	0.1195	0.0042
99536.46	0.988	0.024	0.835	0.021	0.540	0.014	0.1337	0.0045
99514.11	0.933	0.024	0.884	0.022	0.557	0.014	0.1521	0.0049
99491.76	0.954	0.024	0.863	0.021	0.560	0.014	0.1519	0.0049
99469.42	0.985	0.025	0.896	0.022	0.581	0.015	0.1559	0.0051
99447.10	0.945	0.023	0.874	0.022	0.541	0.014	0.1410	0.0046
99424.77	0.975	0.024	0.854	0.021	0.532	0.014	0.1317	0.0044
99402.46	0.968	0.024	0.859	0.022	0.560	0.015	0.1407	0.0047
99380.15	0.931	0.023	0.861	0.021	0.541	0.014	0.1215	0.0042
99357.85	0.968	0.024	0.874	0.022	0.530	0.014	0.1269	0.0044
99335.55	0.930	0.023	0.847	0.021	0.524	0.014	0.1250	0.0043
99313.27	0.991	0.025	0.856	0.022	0.521	0.014	0.1220	0.0043
99290.99	0.973	0.024	0.865	0.021	0.507	0.013	0.1194	0.0042
99268.72	0.965	0.024	0.863	0.022	0.518	0.014	0.1140	0.0041
99246.46	0.954	0.024	0.858	0.021	0.500	0.013	0.1057	0.0039
99224.20	0.944	0.024	0.829	0.021	0.510	0.014	0.1090	0.0040
99201.96	0.919	0.023	0.829	0.021	0.515	0.014	0.1053	0.0039
99179.71	0.995	0.025	0.866	0.022	0.522	0.014	0.1174	0.0042
99157.48	0.976	0.024	0.851	0.021	0.496	0.013	0.1067	0.0040
99135.26	0.945	0.024	0.842	0.021	0.492	0.013	0.1040	0.0039
99113.04	0.921	0.023	0.804	0.020	0.467	0.012	0.0988	0.0037
99090.83	0.977	0.025	0.886	0.022	0.528	0.014	0.1118	0.0041
99068.63	0.979	0.024	0.886	0.022	0.493	0.013	0.1134	0.0041
99046.43	0.926	0.023	0.859	0.022	0.523	0.014	0.1187	0.0042
99024.24	0.950	0.024	0.839	0.021	0.487	0.013	0.1044	0.0039
99002.06	0.949	0.024	0.832	0.021	0.486	0.013	0.1086	0.0040
98979.88	0.922	0.023	0.822	0.020	0.478	0.013	0.1061	0.0039
98957.72	0.917	0.023	0.830	0.021	0.486	0.013	0.1147	0.0041
98935.56	0.962	0.024	0.851	0.022	0.514	0.014	0.1266	0.0044
98913.41	0.948	0.024	0.838	0.021	0.509	0.013	0.1468	0.0048
98891.27	0.945	0.024	0.890	0.022	0.573	0.015	0.1707	0.0053
98869.13	0.972	0.025	0.893	0.022	0.578	0.015	0.1836	0.0056
98847.00	0.957	0.024	0.868	0.022	0.592	0.015	0.1857	0.0056
98824.88	1.013	0.026	0.959	0.024	0.620	0.016	0.1927	0.0060
98802.77	0.955	0.024	0.872	0.022	0.569	0.014	0.1642	0.0051
98780.66	0.960	0.024	0.881	0.022	0.603	0.015	0.1665	0.0053
98758.56	0.961	0.024	0.892	0.022	0.568	0.015	0.1633	0.0052
98736.47	0.981	0.024	0.866	0.022	0.558	0.014	0.1470	0.0048
98714.39	0.952	0.024	0.867	0.022	0.568	0.015	0.1436	0.0048

INTERNAL DISTRIBUTION

- | | | | |
|--------|---------------------------|--------|---|
| 1-3. | L. S. Abbott | 54. | R. W. Peelle |
| 4. | G. T. Chapman | 55. | F. G. Perey |
| 5-9. | G. de Saussure | 56. | R. B. Perez |
| 10. | J. K. Dickens | 57. | E. G. Silver |
| 11. | F. C. Difilippo | 58. | R. R. Spencer |
| 12. | C. Y. Fu | 59. | M. L. Tobias |
| 13. | H. Goldstein (consultant) | 60. | J. H. Todd |
| 14. | R. Gwin | 61. | H. Weaver |
| 15. | N. W. Hill | 62. | C. R. Weisbin |
| 16. | R. W. Ingle | 63. | L. W. Weston |
| 17. | C. H. Johnson | 64. | R. Q. Wright |
| 18. | E. H. Kobisk | 65. | A. Zucker |
| 19. | D. C. Larson | 66. | P. Greebler (Consultant) |
| 20. | R. L. Macklin | 67. | W. W. Havens, Jr. (consultant) |
| 21. | F. C. Maienschein | 68. | A. F. Henry (consultant) |
| 22. | A. G. Mitchell | 69. | R. E. Uhrig (consultant) |
| 23. | G. L. Morgan | 70-71. | Central Research Library |
| 24-53. | D. K. Olsen | 72. | ORNL Y-12 Technical Library
Document Reference Section |
| | | 73-74. | Laboratory Records Department |
| | | 75. | ORNL Patent Office |
| | | 76. | Laboratory Records (RC) |

EXTERNAL DISTRIBUTION

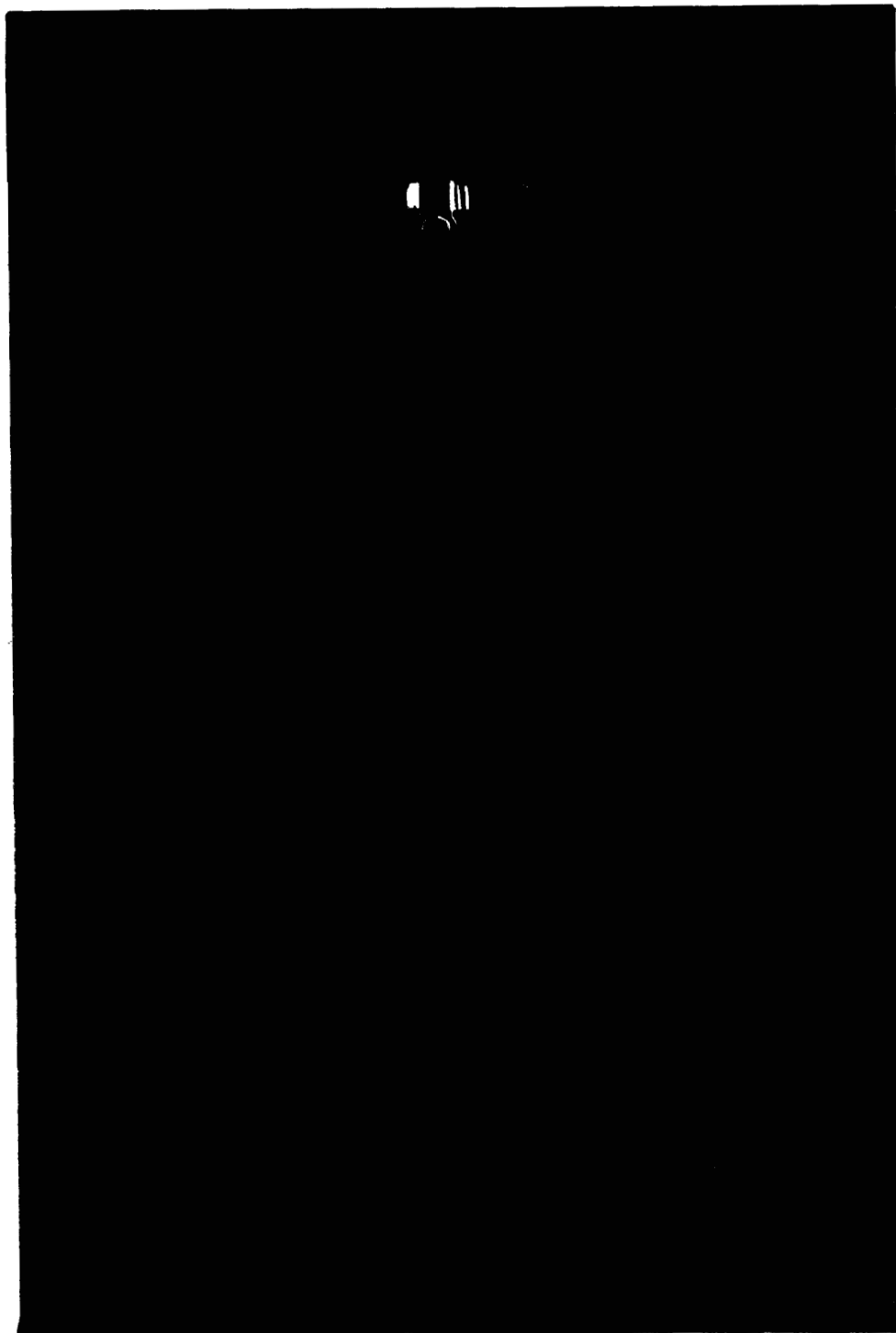
77. USERDA Oak Ridge Operations, Research and Technical Support Division, P. O. Box E, Oak Ridge, Tennessee 37830: Director
78. USERDA Oak Ridge Operations, Reactor Division, P. O. Box E, Oak Ridge, Tennessee 37830: Director
- 79-80. USERDA Division of Reactor Research and Development, Washington, DC 20545: Director
- 81-369. For distribution as shown in TID-4500 Distribution Category UC-79d, Liquid Metal Fast Breeder Reactor Physics - Base (62 copies - ENDF distribution)



150-m MEASUREMENT OF 0.880- to 100.0-keV NEUTRON TRANSMISSIONS
THROUGH FOUR SAMPLES OF ^{238}U

D. K. Olsen, G. de Saussure, R. B. Perez
F. C. Difilippo, R. W. Ingle, and H. Weaver

MICROFICHE ENCLOSED



UNITED STATES DEPARTMENT OF ENERGY
P. O. BOX 62
OAK RIDGE, TENNESSEE 37830
OFFICIAL BUSINESS
PENALTY FOR PRIVATE USE, \$300

POSTAGE AND FEES PAID
UNITED STATES
DEPARTMENT OF ENERGY



Brookhaven National Laboratory ENDF
ATTN: Dr. Charles L. Dunford
National Nuclear Data Center
Building 197
Upton, NY 11973

PRINTED MATTER - BOOKS